

HU ISSN 1785-6892 in print
HU ISSN 2064-7522 online

DESIGN OF MACHINES AND STRUCTURES

A Publication of the University of Miskolc

Volume 11, Number 1



Miskolc University Press
2021

EDITORIAL BOARD

- Á. DÖBRÖCZÖNI
Editor in Chief
Institute of Machine and Product Design
University of Miskolc
H-3515 Miskolc-Egyetemváros, Hungary
machda@uni-miskolc.hu
- Á. TAKÁCS
Assistant Editor
Institute of Machine and Product Design
University of Miskolc
H-3515 Miskolc-Egyetemváros, Hungary
takacs.agnes@uni-miskolc.hu
- R. CERMAK
Department of Machine Design
University of West Bohemia
Univerzitní 8, 30614 Plzen, Czech Republic
rcermak@kks.zcu.cz
- B. M. SHCHOKIN
Consultant at Magna International Toronto
borys.shchokin@sympatico.ca
- W. EICHLSEDER
Institut für Allgemeinen Maschinenbau
Montanuniversität Leoben,
Franz-Josef Str. 18, 8700 Leoben, Österreich
wilfrid.eichlseder@notes.unileoben.ac.at
- S. VAJNA
Institut für Maschinenkonstruktion,
Otto-von-Guericke-Universität Magdeburg,
Universität Platz 2, 39106 Magdeburg, Deutschland
vajna@mb.uni-magdeburg.de
- P. HORÁK
Department of Machine and Product Design
Budapest University of Technology and Economics
horak.peter@gt3.bme.hu
H-1111 Budapest, Műegyetem rkp. 9.
MG. ép. I. em. 5.
- K. JÁRMAI
Institute of Materials Handling and Logistics
University of Miskolc
H-3515 Miskolc-Egyetemváros, Hungary
altjar@uni-miskolc.hu
- L. KAMONDI
Institute of Machine and Product Design
University of Miskolc
H-3515 Miskolc-Egyetemváros, Hungary
machkl@uni-miskolc.hu
- GY. PATKÓ
Department of Machine Tools
University of Miskolc
H-3515 Miskolc-Egyetemváros, Hungary
patko@uni-miskolc.hu
- J. PÉTER
Institute of Machine and Product Design
University of Miskolc
H-3515 Miskolc-Egyetemváros, Hungary
machpj@uni-miskolc.hu

CONTENTS

<i>Alsardia, Talal – Lovas, László – Ficzer, Péter:</i> Prototype for fit investigations	5
<i>Drágár, Zsuzsa – Kamondi, László:</i> The effect of the contact zone of cylindrical helical gears on the meshing and some considerations for determining its shape.....	16
<i>Kiss, Dániel – Szilágyi, Attila:</i> Mechanical analysis of an auxiliary table with composite structure.....	27
<i>Kiss, Dániel – Szilágyi, Attila:</i> Case study: design of a vacuum gripper.....	34
<i>Kiss, Lotár László – Takács, György:</i> Additive metal printing machine tool.....	39
<i>Kmetz, Barbara – Takács, Ágnes:</i> Designing a filament recycling extruder.....	46
<i>Szabó, Kristóf:</i> Steps of generative design in integrated CAD systems	53
<i>Szabó, Kristóf:</i> Application of topological methods.....	59

PROTOTYPE FOR FIT INVESTIGATIONS

TALAL ALSARDIA¹ – LÁSZLÓ LOVAS² – PÉTER FICZERE³

*BME Department of Vehicle Elements and Vehicle Structure Analysis
1111-Budapest*

¹*alsardia@edu.bme.hu, ²lovas.laszlo@kjk.bme.hu, ³ficzere.peter@kjk.bme.hu*
³*ORCID azonosító: 0000-0003-3207-5501*

Abstract: Nowadays, additive manufacturing is a powerful tool and promising technology both for manufacturing and educational purposes. This work aims to present a case study of using 3 dimensional (3D) printing technology for fit investigations. It describes the creation of a physical model (prototype) by using the Fused Deposition Modeling (FDM) method. The prototype of two plates was made to perform an inspection how the prototype fits with other components.

Keywords: *additive manufacturing, Fused Deposition Modeling, fit investigations, rapid prototyping*

1. INTRODUCTION

Additive manufacturing (AM) is defined as the process of joining material to make parts from 3D model data. The real part is built layer by layer. This process is the opposite of the subtractive manufacturing and formative manufacturing methodologies. The 3D-Printing technology is the “fabrication of objects through material deposition using a print head, nozzle, or another printer technology” [1]. The history of AM [2], [3] begins at 1980 when Hideo Kodama made the first 3D printing patent application. He invented a prototyping system based on the hardening of photopolymer material with ultraviolet (UV) light. Three years later, an American engineer Charles Hull, co-founder of the 3D Systems company, invented the first commercial rapid prototyping technology based on the stereolithography (SLA). This machine uses the .stl file format as basic data source for the printing process. The patent dates of 1986. Carl Deckard, in 1987, invented another printing process that uses the laser as the power source for sintering the material powder, known as the selective laser sintering (SLS) process. In 1988, 3D Systems put on the market the first 3D printer for rapid prototyping called SLA-1. In 1989, the “Fused Deposition Modeling” (FDM) process was presented, discovered by Scott and Lisa Crump. In this process, a spool of thermoplastic rope, called filament is pressed in a heated printer head. The movement of this head is controlled by a computer to create the desired geometry of an object layer by layer. In the same year, two well known companies were founded: Stratasys Inc. by Crump in the USA, and “Electro-Optical System” (EOS) GmbH, by Hans Langer in Germany. The process known as “Laser Additive Manufacturing”

(LAM) was developed in 1997 by the Aero Met company, which is a part of MTS Systems Corp. The LAM process uses a high-powered laser for fusing powdered titanium. In 1999, the Institution of Wake Forest for Regenerative Medicine, realized successfully the first 3D printed organ transplantation in a patient body. In 2005, Dr. Adrian Bowyer started an open design project called “RepRap” an abbreviation for Replicating Rapid prototype. RepRap project aimed to develop a 3D printer that can produce most of its own components. Based on this concept, the “Darwin” 3D printer became available in 2008 at a commercial level. The price of an FDM 3D printer fell below 1,000\$ since the patent expiration in 2009. In the same year, 3D printers using materials like “Poly-lactic Acid” (PLA) and “Acrylonitrile Butadiene Styrene” (ABS) were available for consumers, as well as an online library of model files that can be used by 3D printers. In 2011, a complete aircraft and a car body prototype were built using 3D-printing technology.

The “Digital Light Processing” (DLP) printing process was presented in 2012. This process uses a projector for curing a photopolymer resin. In 2015, a 3D bio-printer technology was introduced to the market using a specific type of bio-ink. *Figure 1* illustrates the general classification of AM processes based on the state of the raw material used in this technology. Nowadays there are more than 170 3D-printer manufacturers, including a wide range of applications of this technology in a large variety of sectors like the medical field, engineering industrial application, or educational purposes [4], [5]. In this paper, a detailed case study using FDM printing technology is presented. A 3D-CAD model will be printed, in order to check how the part will fit together with other parts before the manufacturing of the real part in metal.

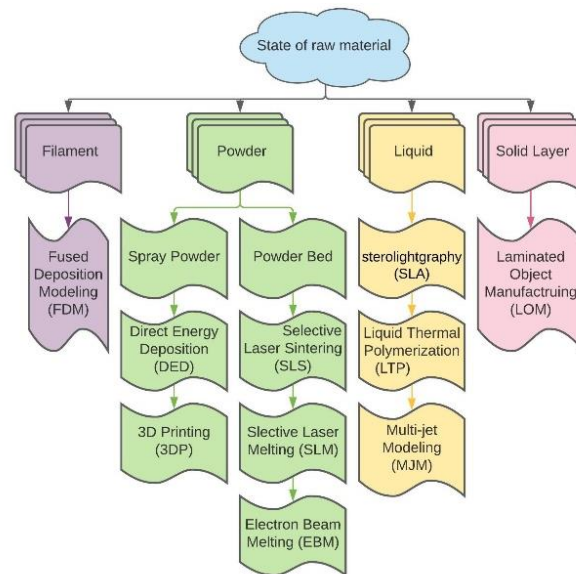


Figure 1

Classifications of AM processes based on the state of used raw materials [6]

2. PROCEDURE

Many road accidents occur due to wheel bolt loosening [7]. *Figure 2* shows a 3D CAD model of a test rig for experimental research on bolted link self-loosening due to vibration.

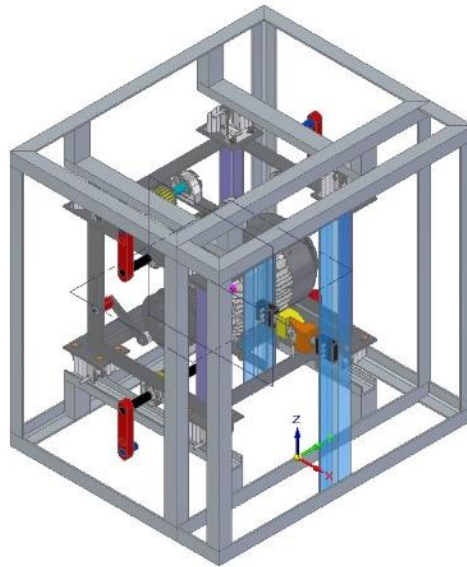


Figure 2. Bolted link test rig

The object of the measurement is a bolted link that compresses two stainless-steel plates together, as shown in *Figure 3*. In the experimental study, different measuring sensors will be mounted on the two plates for data collection. It comes in handy to use 3D-printing technology to facilitate the investigation of the prototype and to study fitting of the parts at low-cost. The flowchart in *Figure 4* outlines the main process steps.

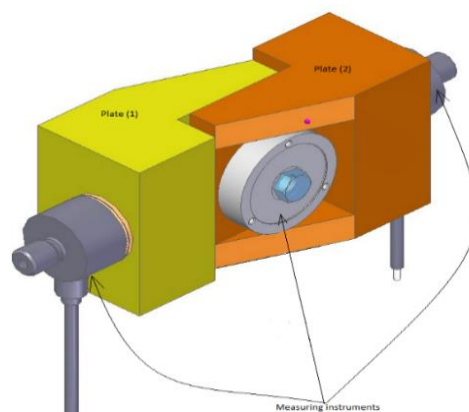


Figure 3. Bolted link

A 3D-printer available at our department is used for printing the two plates. The printer is a Zortrax M200 3D-printer using ABS material. The standard printing parameters of the machine were applied: the ABS material was extruded at 250 °C at a speed of 50 mm/sec with a heated bed surface of 60 °C. The following sections will present further details related to the printing process.

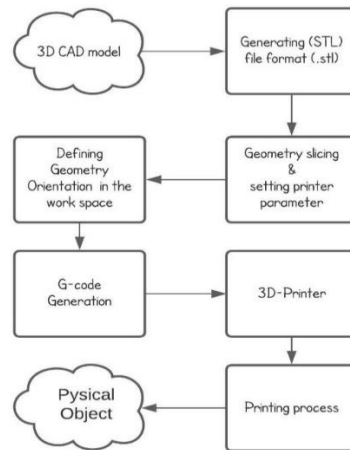


Figure 4. 3D-Printing steps

2.1. Prototype for fit investigations

3D printing or other rapid prototyping processes have been used for a long time to produce object prototypes. Although CAD models are excellent in geometry representation, it is not always clear how efficiently a model fits and satisfies the prescribed functions until you have a real part based upon a CAD model.

The investigated 3D model consists of two plates. One of these plates shown in *Figure 5*. The geometry was built in a commercial CAD environment. The software exported the model in the required .stl format, and another program performed the slicing of the geometry for the printing process.

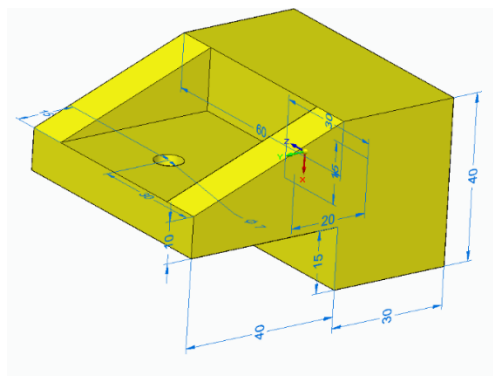


Figure 5. 3D-CAD model of the plate

2.2. STL file conversion

The data describing a 3D-CAD model is packed in a file that contains the desired geometry surface information. To perform the printing process by the 3D printer, a specific file format is needed. This file type is known as “Surface Tessellation Language” or “Standard Triangular Language” or simply STL file. 3D Systems company introduced this file format in 1987. Our CAD environment, the Solid Edge software generates the STL file format using a built-in function, after setting the parameters as shown in *Figure 6*. An STL file consists essentially of a long list of triangles that together cover the surface of the object as shown in *Figure 7*. It is relatively simple to generate an STL file format for both ASCII and binary file versions [8].

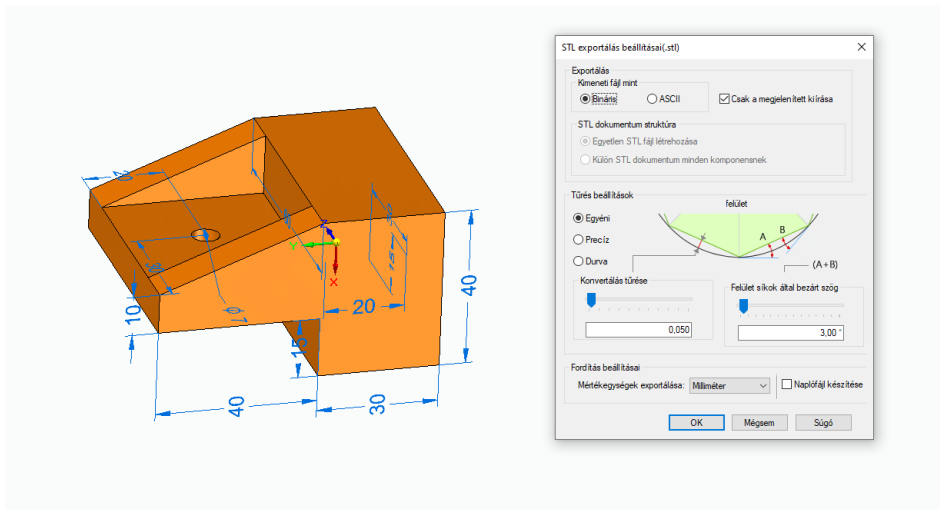


Figure 6. Parameters for generating .stl file format

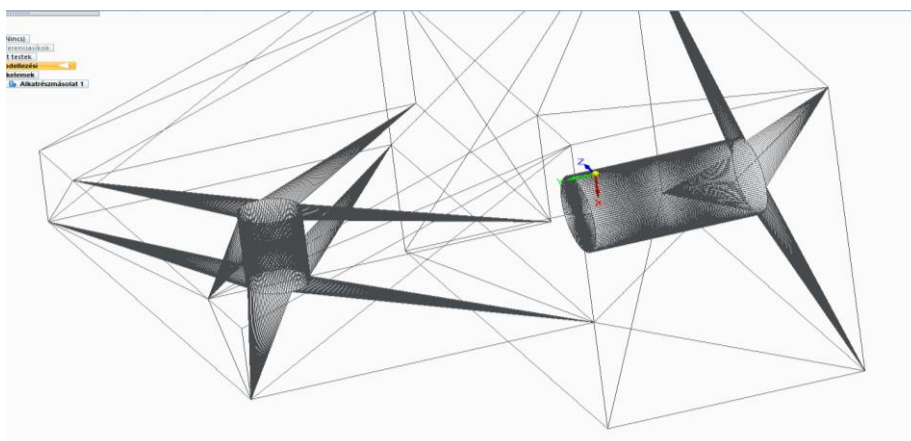


Figure 7. Model representation using (.stl) file format

2.3. Orientation

In this step, the main task is to figure out the best orientation of the model on the 3D printer platform during the printing process. We have to select which face of the geometry is the base, giving the orientation of the layers. It is good practice to choose such geometry orientation that minimizes the need for support material. If there are hollow features in the shape, then there are two options. Either the hollow features are laid down perpendicularly to the base surface, or the 3D printer will print them in any position by bridging across geometrical gaps. In our prototype case, the hollow cylinder feature is an example of that, where the 3D-printer bridged the cylindrical gaps. *Figure 8* shows the selected orientation for the plates during the printing process.

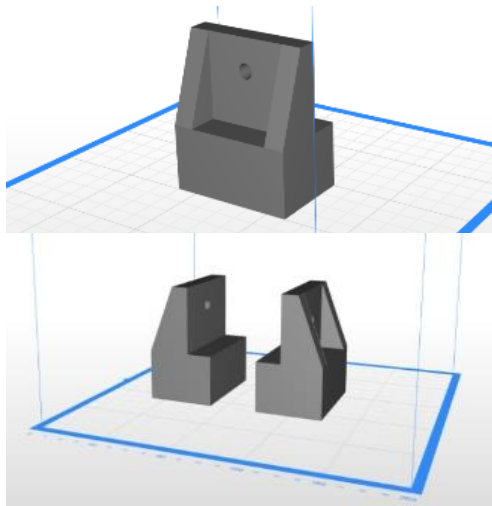


Figure 8. Model orientation on the platform

A 3D-printer can not use a direct 3D-CAD model file format. A conversion into another file format is needed that the 3D printer can understand. 3D printers build the part layer by layer, thus, the division of the model into printable layers is required. The first conversion results a 3D model in an easy to handle .stl format. Then, the separation into layers named slicing is realized, based on the selected geometry dimensions and the capability of the 3D printer itself [8].

2.4. Printing parameter setup

The parameters governing the printing process were as follows. The 3D-printer was a Zortrax type M200, the printing material an ABS filament material, and the standard default parameters of the 3D printer were used, with automatic support creation. The ABS material was extruded at 250 °C with honeycomb pattern, with 20% filling option at a speed of 50 mm/sec and with heated bed surface at 60 °C. *Table 1* summarizes the 3D printer parameter settings, and *Figure 9* shows the set of printing parameters.

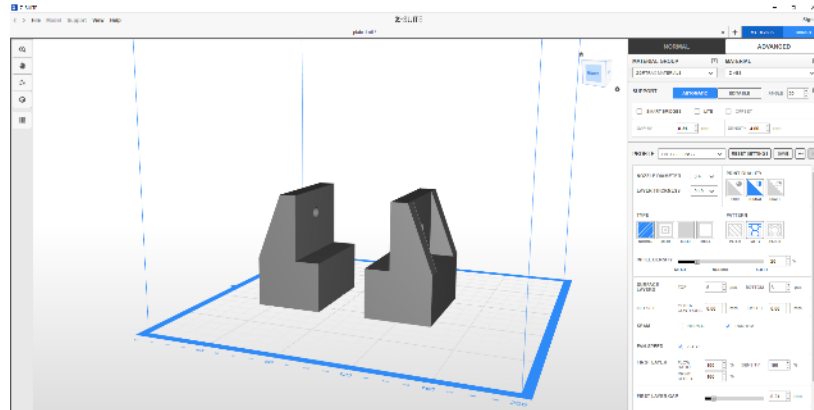


Figure 9. 3D-Printer parameter set up

Table 1
Printing parameters

	Parameter	Setting
1	Nozzle diameter	0.4 mm
2	Layer thickness	0.19 mm
3	Infill pattern	honeycomb
4	Infill density	20%
5	Speed	50 mm/sec
6	Platform surface temperature	60 °C

After setting the 3D-printer parameters, there is an option for visualizing the printing process versus time as a print preview. Using that, the time estimation at a different level of process completions can be determined with a 3D preview based on the defined parameters, as shown in Figures 10–13.

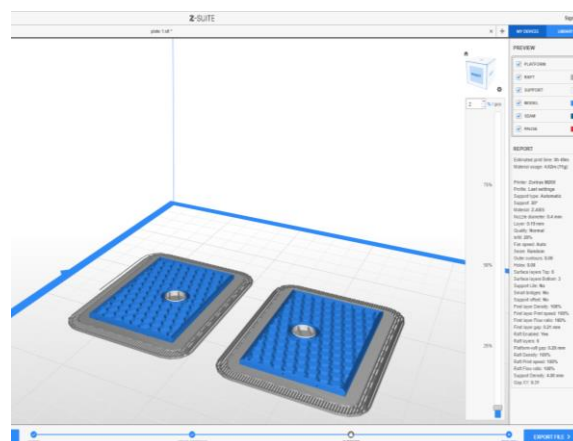


Figure 10. Printing process preview at 2% readiness

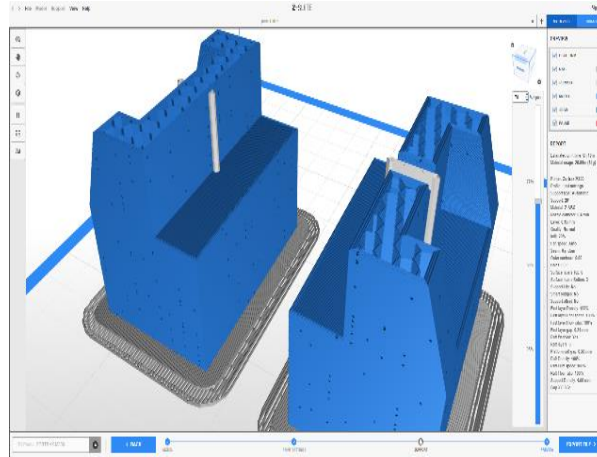


Figure 11. Printing process preview at 70% readiness

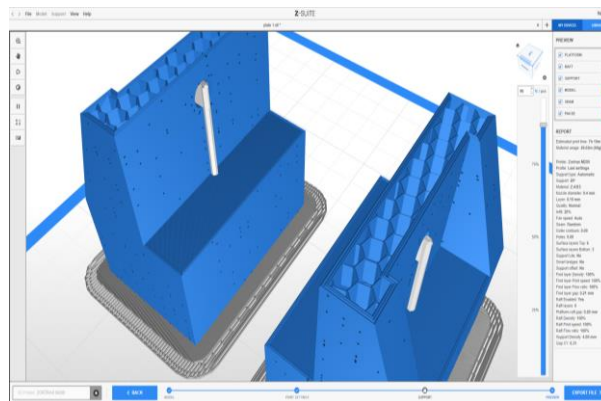


Figure 12. Printing process preview at 90% readiness

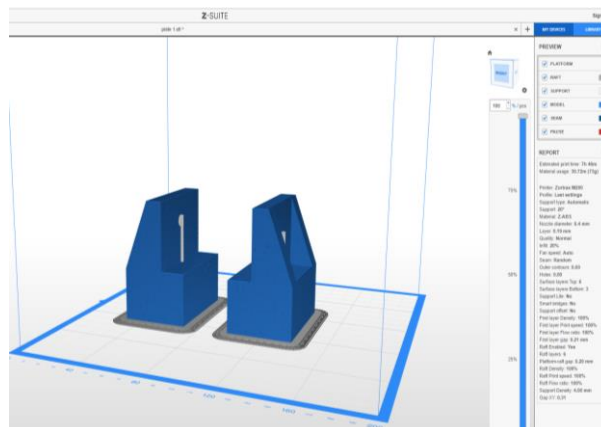


Figure 13. Printing process preview at 100% readiness

2.5. G-code to the printer

The G-code is a simple programming language used to control the printing process and describe the nozzle path in the 3D printer. The code for the printing of the part is created automatically after the generation of the slices. In our case, the generated code is uploaded to the 3D printer using an SD card interface. The printer micro-controller follows the G-code during the printing execution process. Typical G-code functions include commanding an extruder to heat to a specific temperature, instructing the printer to pause until the extruder reaches the desired temperature, moving the extruder to given (x, y, z) position, and carrying out other related tasks.

3. CONCLUSION

Before manufacturing a new part, it is often required to check the geometric fitness of a designed geometry. To reach this goal, 3D printing technology was selected due to the advantages of the technology: speed, low cost, and flexibility.

Figures 14–15 show the printing process at different time steps.

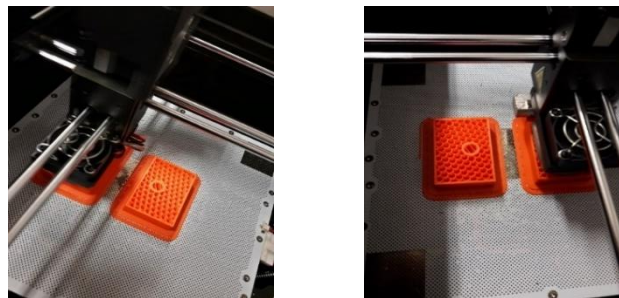


Figure 14. Printing progress

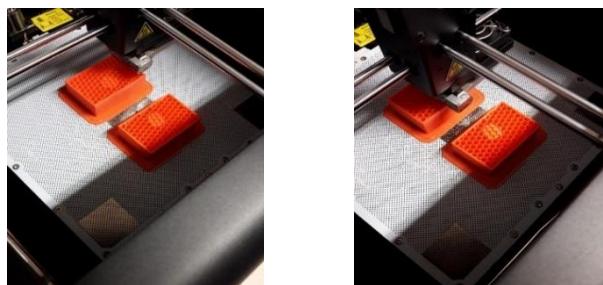


Figure 15. Printing progress

A Zortrax M200 3D printer was used for printing the 3D model of our part, using ABS material. We followed the steps of the manufacturing procedure from CAD model to the ready pieces with the previously defined parameters. *Figure 16* shows the final printed model. The time needed for printing both plates was 7 hours and 46

minutes, while using 37 g of ABS material. In this approach, the model's physical properties were not a point of interest. *Figure 17* shows the final assembly of the geometry after the 3D-printing process. The manufactured geometry shows good agreement with the expected target, and no modifications are needed to enhance the structure compatibility with other parts.

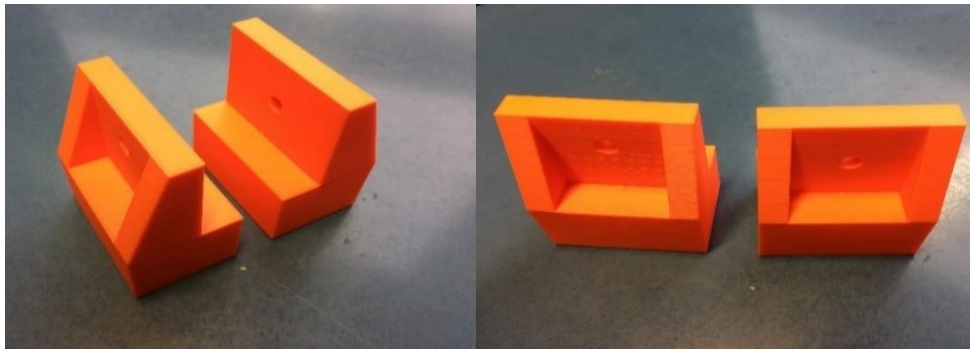


Figure 16. The printed model

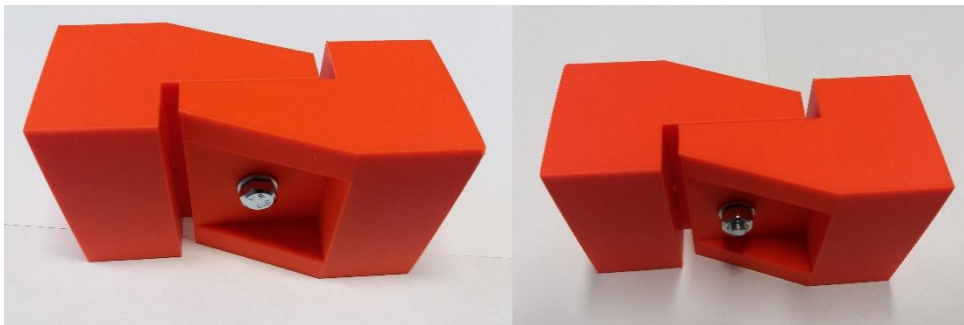


Figure 17. Assembled joint

REFERENCES

- [1] ISO-ASTM: *ISO-ASTM 52900:2015(en), Additive manufacturing – General principles – Terminology*. 2015, <https://www.iso.org/obp/ui/#iso:std:iso-astm:52900:ed-1:v1:en> (accessed Dec. 12, 2020).
- [2] González, C. M.: *Infographics: The History of 3D Printing*, ASME. 2020, <https://www.asme.org/topics-resources/content/infographic-the-history-of-3d-printing> (accessed Dec. 24, 2020).
- [3] Wohlers, T. – Gornet, T.: *History of additive manufacturing*. Wohlers Report, 2014.
- [4] Ford, S. – Minshall, T.: Invited review article: Where and how 3D printing is used in teaching and education. *Additive Manufacturing*, Vol. 25, January 2019, pp. 131–150, 2019, DOI: 10.1016/j.addma.2018.10.028.

-
- [5] Ficzer, P. – Horváth, Á. M. – Sipos, T.: Elalvások balesetek csökkentési lehetősége additív gyártási eljárással fejlesztett kapszulák segítségével. *Közlekedéstudományi szemle*, Vol. 70, Nr. 1, 2020, pp. 77–85, DOI:10.24228/KTSZ.2020.1.3.
- [6] Korner, M. E. H. – Lambán, M. P. – Albajez, J. A. – Santolaria, J. Ng Corrales, L. C. – Royo, J.: Systematic Literature Review : Integration of Additive Manufacturing and Industry 4.0. *Metals*, Vol. 10, Nr. 8, pp. 4–7, 2020, DOI: 10.3390/met10081061.
- [7] Sipos, T.: Coherence between Horizontal and Vertical Curves and the Number of the Accidents. *Periodica Polytechnica Transportation Engineering*, Vol. 42, Nr. 2, 2014, pp. 167–172., DOI: 10.3311/PPtr.7403.
- [8] Horvath, J.: *Mastering 3D printing: modeling, printing, and prototyping with reprop-style 3D printers*. Apress Media LLC, California, 2014.

THE EFFECT OF THE CONTACT ZONE OF CYLINDRICAL HELICAL GEARS ON THE MESHING AND SOME CONSIDERATIONS FOR DETERMINING ITS SHAPE

ZSUZSA DRÁGÁR¹ – LÁSZLÓ KAMONDI²

^{1,2}*University of Miskolc, Institute of Machine and Product Design
3515 Miskolc-Egyetemváros*

¹*machdzs@uni-miskolc.hu, ²machkl@uni-miskolc.hu*

¹<https://orcid.org/0000-0003-2028-7718>

²<https://orcid.org/0000-0002-0883-4304>

Abstract: The study deals with the meshing characteristics of cylindrical helical external gear pairs. The gear pairs, following the nowadays' strength and quality requirements are becoming ever smaller. Accuracy in the background also attracts the importance of vibration and noise reduction. The inclined tooth meshing, in contrast to the straight tooth, due to the specificity of its zone of contact, is the subject of this study. This is of special importance because the meshing stiffness varies for one to more teeth pairs, the meshing contact lines are of continuously varying length during meshing, and as a consequence load sharing and distribution is changing with. This paper deals with the zone of contact and its geometric modification in order to light on a new type of vibrational excitation.

Keywords: *zone of contact, meridian, top land modification*

1. DEVELOPMENTAL MOTIVATORS OF THE MESHING NATURE OF CYLINDRICAL HELICAL GEARS

Technical progress in moving structures has always shown that developers cannot avoid that the structures they build includes a toothed element in the drive chain. The drive chains used have and continue to have a wide variety of shapes, from the simplest to the most advanced solutions used nowadays. This diversity was reflected in the materials used, the teeth geometry and the expected accuracy [1]. The design of the tooth has undergone a long development from, through the carved tooth, to the fine finished tooth form [1, 9].

The development of military technology (on the land, in the air, under water), in parallel with the development of terrestrial civilian means of transport, required more and more precise elements of the drive chains. This was motivated on the one hand by the extension of service life, on the other hand by safety and on the third hand by recognizability. In terms of service life, it can be observed that the gears require less and less care. The quality of the materials used and the refinement of strength calculation and inspection procedures also support safety [2].

Recognition is already a more complex problem. The gear transmission was initially expected to be reliable, today it is expected to be also quiet. In special cases the unidentifiability of the drive chain can be also a requirement, especially by the military equipment.

The development today is clearly directed as follows:

- the toothed element connection in the drive chains cannot be avoided,
- the accuracy of the motion mapping, thus reducing the variation of the angular velocity to an absolute minimum,
- the vibration-generating sources of the meshing shall be minimized,
- the coupling of the toothed pair should have less acoustic emission in order to become more difficult to recognize it.

2. THE CONTACT ZONE AS THE LOCATION OF THE MESHING IS THE SOURCE OF THE PROBLEMS

The mapping of the contact zone is well defined and described in all gear literature [3, 4, 5, 10], yet let us consider it in a figure (*Figure 1*). The tooth pairs are meshing in a field ($AEA'E'□$). Points A and E on the line of action are designated by the head cylinders. The common width (b) of the gear body determines the points A' and E', thus the theoretical zone of the meshing becomes the rectangle $AEA'E'$.

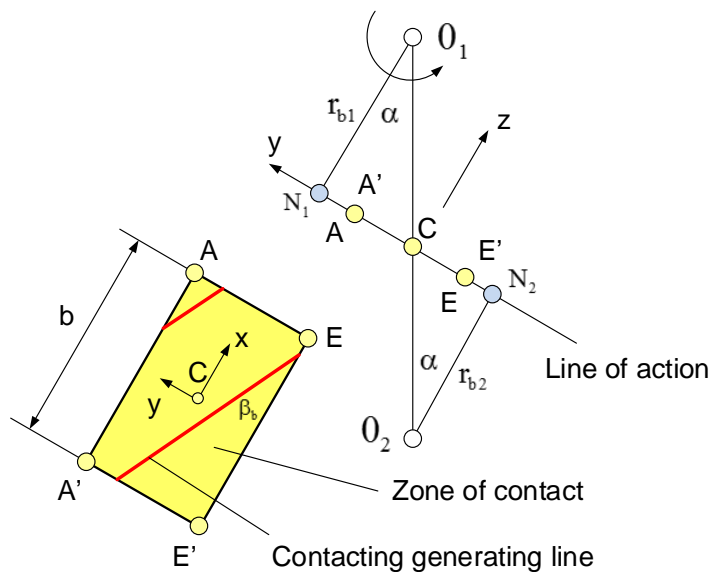


Figure 1

Interpretation of the uncorrected contact zone

The meshing begins at point A and proceeds to point E'. It can be observed that, depending on the base pitch, more than one pair of teeth can connect at the same

time, which is also indicated by the number of contacting generating lines. The individual length of the instantaneous contacting generating lines and their sum also change continuously in the zone of contact. These lengths are determined by purely geometrical features. The meshing pairs of teeth also carry a load, the consequence of which is that their stiffness – considering them individually or summarized – is constantly changing. At the same time the load distribution between and along the contacting generating lines also changes [5, 6]. The movement in the zone of contact and the load conditions can be significantly affected by the manufacturing and assembling errors, as well by the errors resulting from the elastic deformation of the drive.

The effects of the errors mentioned above result in vibrations and acoustic phenomena. Research in recent decades has focused on understanding these phenomena, on exploring their impact, and on reducing their influence [7, 13, 14].

3. POSSIBILITIES OF DEFINING THE CONTACT ZONE

The meshing characteristics of helical cylindrical gears are affected by the shape (appearance) of the zone of contact. This statement is of great significance because here appears the characteristic effect and source that determines the connection of each gear.

When designing the gear, a basic geometry is defined, which records the basic input data (gear ratio, basic profile, module, number of teeth), the diameter of the characteristic circles (cylinders), the shaft distance, and the common tooth width. The top land of the teeth is a cylinder whose meridian section is a line parallel to the axis. The zone of contact that can be mapped from this is a rectangle (*Figure 1*). If we want to form a different geometric shape in addition to the regular rectangular shape for some expedient consideration, three possible ways of defining the zone of contact are conceivable. Variants can be created through keeping the meridian section of the theoretical head cylinders unchanged or changing them. The basic cases are as follows:

- the meridian section of the top land surface remains a line parallel to the axis of rotation (*Figure 1*), i.e. a rectangular zone,
- the meridian of the top land surface is determined using straight lines or a set of higher order curves (direct method),
- the complete rectangular zone of contact is modified first and the meridian curve or curves of the top land surface are determined from this (indirect method).

The algorithm for determining the possible solutions is illustrated in *Figure 2*, which also points the necessary modification of the drawings of gears.

4. ZONE OF CONTACT GENERATED BY THE MERIDIAN OF TOP LAND SURFACE, INDIRECT PROCEDURE

The indirect solution of the mapping of the contact zone means starting from the given geometry of the meshing gears and not touching directly the zone of contact. The actual geometry here means that all the geometrical data of the gears are known, as well the dimensions related to the center distance. *Figure 3* shows the mapping of

the contact zone, starting first from an unmodified top land surface, followed by the mapping after the modification of the top and surfaces, using the indirect procedure. The starting point for the mapping is to disregard the modification of the meridian of the head cylinder. A regular rectangular zone of contact can then be mapped. The geometric basis of this is known from several literature [3, 5]. This is determined on the one hand by the geometric dimensions from the basic geometry:

- normal module,
- number of teeth,
- base profile angles (working, supporting),
- addendum height coefficient,
- clearance coefficient,

on the other hand, the connection characteristics:

- shaft distance,
- addendum modification coefficients,
- addendum circles (uncorrected case),
- dedendum circles,
- tooth width.

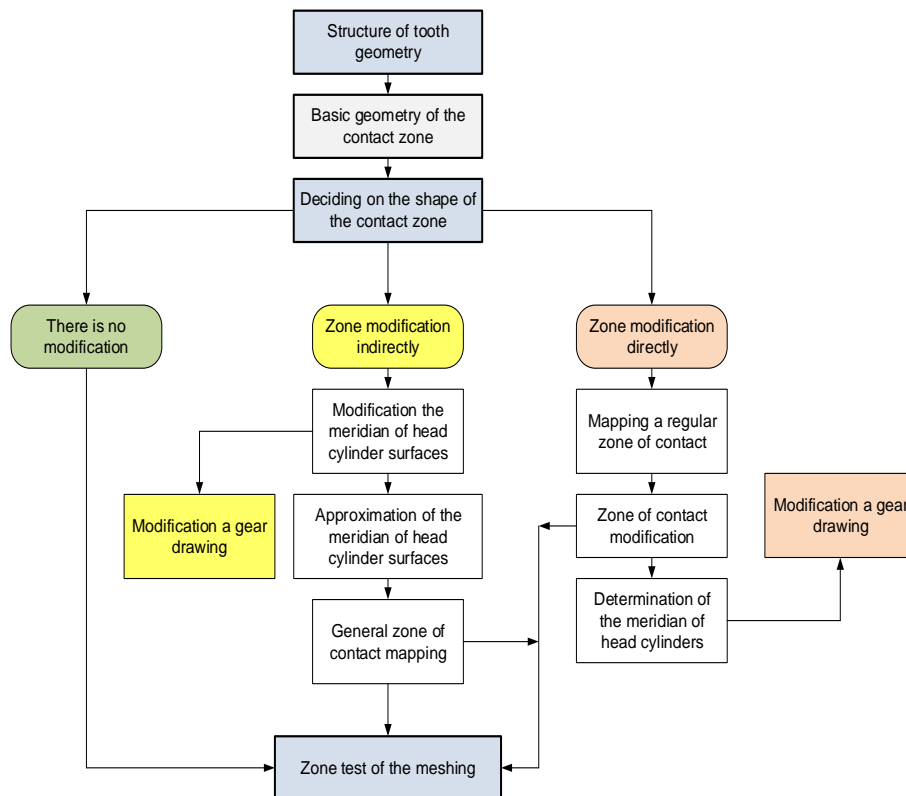


Figure 2

Possible cases of defining the zone of contact (own figure)

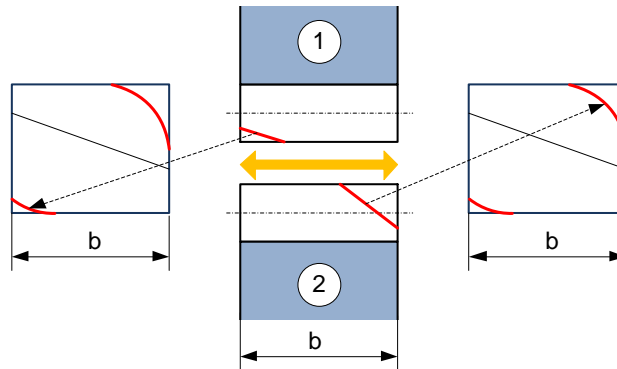


Figure 3

The top land surface generates the zone of contact, while applying the indirect procedure

The meridian of the top land surface can be modified by breaking the straight line parallel to the axis of rotation, by another straight line or regulus, in a more complex case by a higher order curve. Such possibilities are illustrated in *Figure 4* on a single gear only.

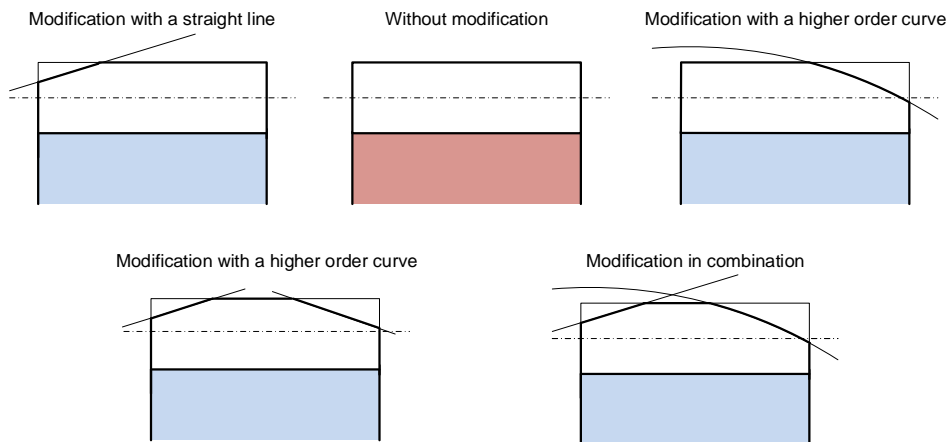


Figure 4

Top land meridian design options

The zone of contact is limited here by the upper and lower zone borders and the common tooth width, as illustrated in *Figure 5*. The top land meridian was modified by taking a straight line for each gear as shown in *Figure 3*. The borders of the contact zone can be determined by the coordinates (x_i^*, r_{i*}) of the points of the meridian curve in the x, y coordinate system, which is connected to the main point C taken in the middle of the common tooth width (*Figures 1 and 5*).

The y coordinates of the zone borders can be determined by *Equations (1) and (4)* as a function of x, whose domain is: $-b/2 \leq x \leq b/2$.

Zone upper border points (red line) are defined by the following equations:

$$y_F^* = \overline{N_2 A^*} - \overline{N_2 C}, \quad (1)$$

$$\overline{N_2 A^*} = \sqrt{\left(\frac{d_{a2}^*}{2}\right)^2 - \left(\frac{d_{b2}}{2}\right)^2}, \quad (2)$$

$$\overline{N_2 C} = \sqrt{\left(\frac{d_2}{2}\right)^2 - \left(\frac{d_{b2}}{2}\right)^2}. \quad (3)$$

Zone lower border points (blue line) are given by:

$$y_A^* = \overline{N_1 C} - \overline{N_1 E^*}, \quad (4)$$

$$\overline{N_1 E^*} = \sqrt{\left(\frac{d_{a1}^*}{2}\right)^2 - \left(\frac{d_{b1}}{2}\right)^2}, \quad (5)$$

$$\overline{N_1 C} = \sqrt{\left(\frac{d_1}{2}\right)^2 - \left(\frac{d_{b1}}{2}\right)^2}. \quad (6)$$

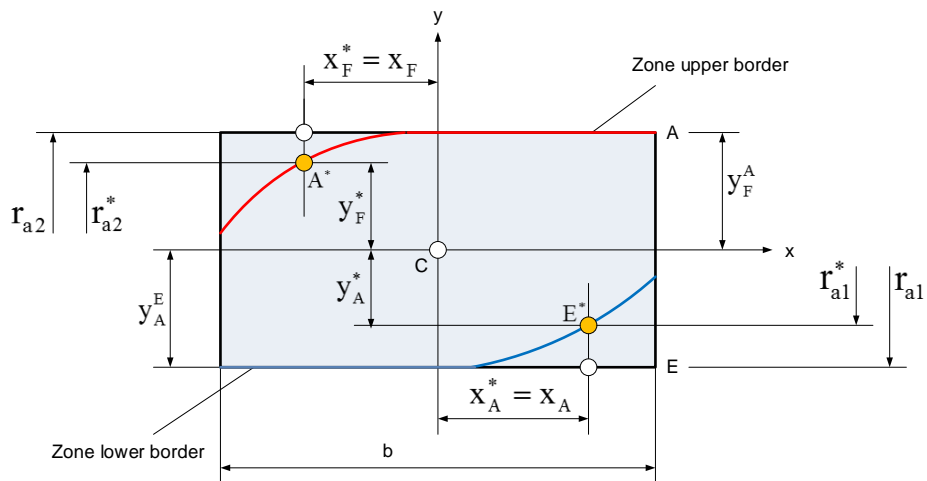


Figure 5
Geometric mapping of the contact zone

In the zone of contact, as shown in *Figure 1*, the contacting generating lines are located according to the inclination of tooth directional angle (β_b) on the base cylinder and thus they traverse in this mode the zone of contact. It can also be seen that the lengths of instantaneous contacting generating lines and their sum also vary. The nature of the change will be influenced by the total tooth width (b) and the shape of the lower and upper zone borders. Here we do not deal with the analytical solution, it will be included in a further presentation.

5. GENERATION OF THE MERIDIAN OF THE TOP LAND SURFACE, DIRECT PROCEDURE

The direct procedure for modifying the contact zone consists in modifying first the regular rectangle zone of contact. The reason for the modification may be to improve a zone property [7, 8]. For example, it may be to reduce the amount of variation of the total length of the contacting generating lines or restrict the migration of tooth forces. *Figure 5* shows, on the one hand, the gears with an uncorrected top land surface and the corresponding regular rectangular zone of contact while by the other hand, it shows the modified contact zone and its effect on the form of the meridians of the gear top land surface.

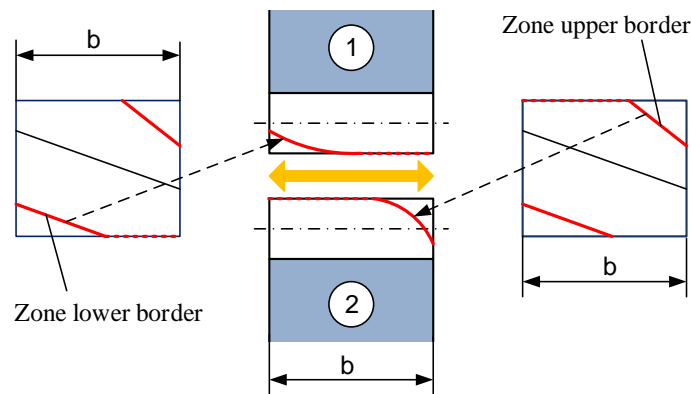


Figure 6

The zone of contact generates the meridian of the top land surface, direct procedure

In the zone on the left, we truncate the zone with a straight line not the full width of the tooth, so we get a new *lower zone border*. That zone border modifies the top land surface of the gear 1, thus determining the shape and expression of the meridian. In the zone on the right side, we have proceeded in a similar manner to determine the *upper zone border* and the meridian of the top land surface of gear 2. Of course, the modification using a straight line is not the unique solution; it can be implemented also through regulus or a higher order curve, resp. a group of curves.

Figure 7 illustrates a modified zone of contact obtained by the direct method. The marked points on the zone borders, are transposed on the top lands as points of the modified meridian curves.

$$r_{a1}^* = \sqrt{\left(\frac{d_{b1}}{2}\right)^2 + (\overline{N_1 E^*})^2} \quad (7)$$

$$\overline{N_1 E^*} = \overline{N_1 C} + |y_A^*|, \quad (8)$$

$$\overline{N_1 C} = \sqrt{\left(\frac{d_1}{2}\right)^2 - \left(\frac{d_{b1}}{2}\right)^2}, \quad (9)$$

and

$$r_{a2}^* = \sqrt{\left(\frac{d_{b2}}{2}\right)^2 + (\overline{N_2 A^*})^2}, \quad (10)$$

$$\overline{N_2 A^*} = \overline{N_2 C} + |y_F^*|, \quad (11)$$

$$\overline{N_2 C} = \sqrt{\left(\frac{d_2}{2}\right)^2 - \left(\frac{d_{b2}}{2}\right)^2}. \quad (12)$$

Figure 8 shows where this point is located on the gears. The point taken at the zone border can be transferred to the gear by Equations (7) to (12) using Figure 1. The relations can be applied for all the points of the lower and upper zone borders with arbitrary x^* coordinate points. It determines the meridians of the top land surfaces, to which can be finally added a fitting function.

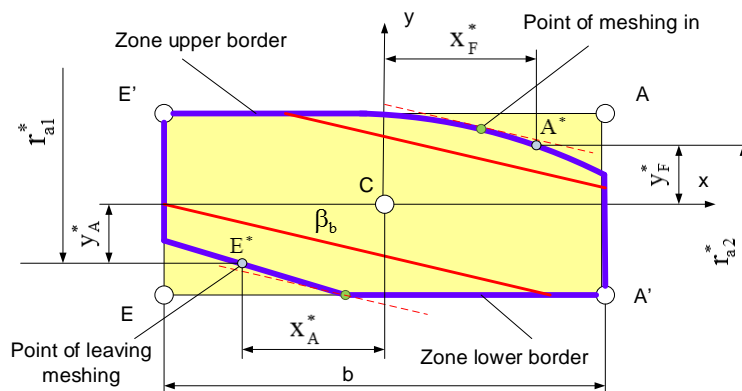


Figure 7. Defining a zone of contact directly

In the zone of contact, the lower and upper zone borders will contain also unaffected segments. The top land surfaces of the gears remain unchanged in the width corresponding to this zone, which is also shown in *Figure 8*.

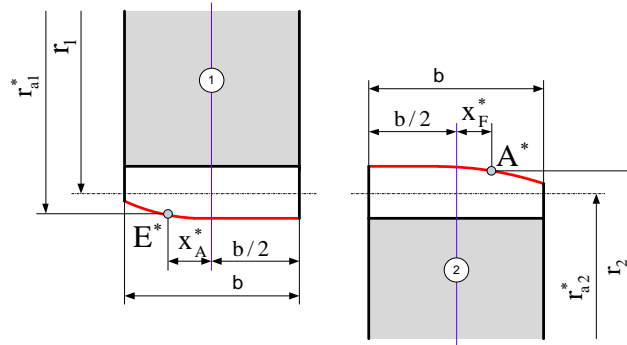


Figure 8
Gears with modified top land surfaces

The corrected tooth top land surface can be provided by machining the wheel bodies before toothing. This is easily feasible in nowadays modern CNC techniques.

6. THE EFFECT OF THE CHANGED CONTACT ZONE ON THE LENGTH OF THE CONTACTING GENERATING LINES

In the zone of contact, the contacting generating lines of the meshing pairs of teeth follow each other at a distance of base pitch in normal section p_{bn} . In the case where the zone of contact is not modified, the length of the contacting generating lines can be determined from the parameters of the contact zone. Examining the pair of teeth entering at point **A** (point of meshing in) and its contacting generating line (*Figure 9*), it can be observed that its length varies continuously till they reach the point of leaving the meshing **E**. This change in length is also influenced by the common tooth width b , which is always the result of a designer decision. The effect of the length variation on the meshing process can be described in dependence with the zone parameter Δy .

The summed contacting generating line results as the sum of each component:

$$L_{\Sigma}(\Delta y) = \sum_{i=1}^{i=n(\Delta y)} L_i(\Delta y). \quad (13)$$

In the design phase, it is expected to reach the maximum load capacity in addition to minimum weight. The defining of the common tooth width also obeys this goal. The literature [1, 3,] was coming here with a recommendation that couldn't be refuted for a long time. According to that, as long the common tooth width is imposed to be an integer multiple of the axial pitch (p_x), the sum of the lengths of the components (contacting generating lines) remains constant and thus torsional excitation can be avoided. This is in fact true, but subsequent research [12, 13] has shown that this

cannot be substantiated, since the common tooth width must be determined from different consideration, because other types of excitations are also present. Subsequent research [7, 8, 11] confirmed this hypothesis that significant results in reducing vibration excitation can be achieved by expedient modification of the contact zone.

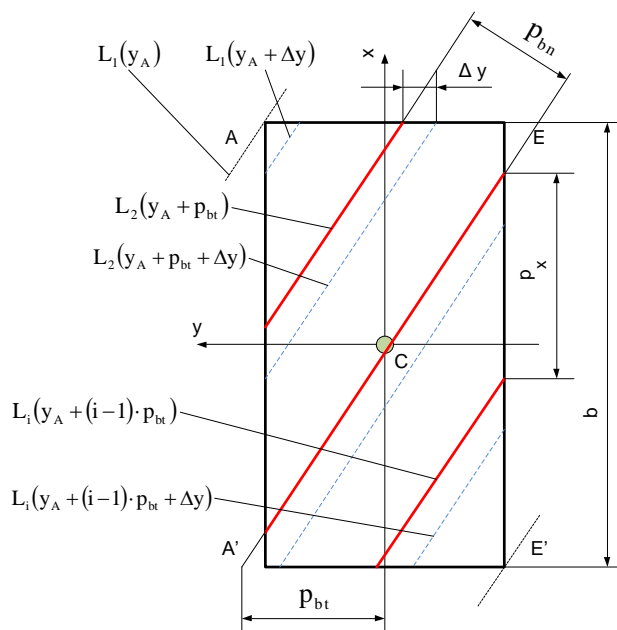


Figure 9

Length change of contacting generating lines

7. CONCLUSIONS, RESULTS

The article points that the well-known powertrain element in the literature, the helical-toothed cylindrical external gear, raises certain questions that, in the context of nowadays manufacturing technology and the charge under the high-quality requirements oblige the designer to meet them. The solution is hiding in the geometry of the contact zone. The results of our study can be summarized as follows:

- the shape of the contact zone does not have to follow the shape of the classic, regular rectangle, well-known from the literature,
- the zone of contact is characterized by the change of the length of the contacting generating lines located inside it, and this depends on the meshing position,
- modifying the shape of the contact zone can be done in two independent ways,
- the reason for the deformation of the contact zone is to reduce the level of vibrations,
- it is not justified to choose a width of the zone of contact (common tooth width) that equals a multiple of the axial pitch.

A further aim of the research is to describe the changes in the zone of contact and their effect on the meshing characteristics.

REFERENCES

- [1] Graf, H. CHR.: *Die Entwicklung der Zahrad-Technik*. Springer-Verlag, Berlin, 1965.
- [2] Debreczeni, D.: *Evolvens, külsőfogazatú, hengeres fogaskerékpárok fogtő teherbírásának és egyfopár merevségének geometriai függősége*. PhD-értekezés, Miskolc, 2021.
- [3] Erney, Gy.: *Fogaskerekek*. Műszaki Könyvkiadó, Budapest, 1983.
- [4] Litvin, F. L.: *A fogaskerékkapcsolás elmélete*. Műszaki Könyvkiadó, Budapest, 1972.
- [5] Niemann, G., Winter, H.: *Maschinenelemente*. Band II, Springer-Verlag, Berlin. 1983.
- [6] Linke, H. – Senf, M.: Breitenlastverteilung bei Verzahnungen-Berechnung und Diskussion von Einflüssen. *Maschinenbautechnik*, Berlin, 32 (1983), 10, pp. 437–444.
- [7] Kamondi, L.: *Ferdefogú hengeres fogaskerékpár kapcsolódásából származó rezgésgerjesztés és a kapcsolómező nagyságának összefüggése*. Egyetemi doktori értekezés, Miskolc, 1986.
- [8] Drágár, Zs. – Kamondi, L.: The role of the tooth shape in powertrains containing gears. *26th International Conference on Mechanical Engineering*, OGÉT 2018, Romania, Targu Mures, 2018, pp. 232–235.
- [9] Roth, K.: *Zahnradtechnik, Band I: Stirnradverzahnungen-Profilverschiebungen, Toleranzen, Festigkeit*. Springer Verlag. 1989.
- [10] Roth, K.: *Zahnradtechnik, Band II: Stirnradverzahnungen-Geometrische Grundlagen*. Springer Verlag, 1989.
- [11] Drágár, Zs. – Kamondi, L.: Tooth Root Stress Calculation for Non-symmetric Tooth Shape. *GÉP*, ISSN 0016-8572, LXIV. évf., 6. szám, pp. 25–28., 2013.
- [12] Attia, A. Y.: Noise of involute helical gears. *Journal of Engineering for Industry*, Vol. 91, No. 1, pp. 165–171., DOI: 10.1115/1.3591505, 1969.
- [13] Ajrapetov, E. L. – Genkin, M. D.: *Dinamika planetarnüh mechanizmov*. Izdatelstvo Nauka, Moscow, 1980.
- [14] Ajrapetov, E. L. – Genkin, M. D.: *Kolebanija mechanizmov sz zubcsatümi peredacsami*. Izdatelstvo Nauka, Moscow, 1977.

MECHANICAL ANALYSIS OF AN AUXILIARY TABLE WITH COMPOSITE STRUCTURE

DÁNIEL KISS¹ – ATTILA SZILÁGYI²

^{1,2}*University of Miskolc, Department of Machine Tools*
3515 Miskolc-Egyetemváros
¹*kiss.daniel@uni-miskolc.hu*
²*szilagyi.attila@uni-miskolc.hu*

Abstract: This paper gives a brief summary on the application on of finite element methods during the design of a component. The solutions of mechanical and thermal problems are demonstrated on the given component. Among the several numerical methods the paper focuses on the FEM. During the article we present the problems, then define mechanical simulations for the possible solution that was designed and the evaluation of the results.

Keywords: *FEM, mechanical, thermal, numerical*

1. INTRODUCTION

When designing machines, all factors related to the accuracy and in-service parameters of the machine must be taken into account. These factors include deformations and vibrations caused by certain thermodynamic and mechanical phenomena. The effect of these should be taken into account already in the planning phase, since in this case it is the most economical to detect errors. Since the device is not physically available in the design phase, these phenomena can be modeled using simulation software [1].

The part to be examined is an auxiliary table with a composite structure, the task of which is to guide two laser devices facing each other with the best possible accuracy. The two laser devices are located on a carriage, which guidance is provided with linear guideways. Such guideways can be purchased as commercial parts for the industry in several different accuracy classes, however, ensuring accuracy depends not only on the properties of these components, but also on the base on which they are mounted. The mechanical properties of this component should be investigated, which will be done by finite element analysis [2], [3].

The laser devices or its guides are generally mounted on optical tables, however, the flatness of optical tables based on catalog data does not meet the accuracy required for roller guideways (0.015 mm) [4], [5]. Therefore, an auxiliary table should be designed that has adequate mechanical accuracy, good rigidity and good thermal properties. In accordance with these requirements, we consider the structure to be optimally designed. Various solutions were developed during the design process,

in which the ribbed aluminum version (*Figure 1*) was discarded due to poor thermal properties, and the steel version was not considered a suitable choice due to its significant weight. As a final solution, a composite design was chosen, which is illustrated in *Figure 2*, in which an aluminum-granite-aluminum bonded structure was used. When designing the composite table, we aimed to create a structure with as low weight as possible and which can perform its functions with maximum static and dynamic rigidity and minimum thermal deformation, taking into account ergonomic principles.



Figure 1. Ribbed structure with aluminium material



Figure 2. Table with composite structure equipped with guideways

The choice of aluminium material is due to the fact that by using a suitable alloy, it will have mechanical properties similar to mild steel materials but have significantly lower weight. The chosen alloy is EN-AW-2014-T6, which is also defined for the simulations. Aluminium alloy EN-AW-7075-T6 has similar properties. Granite was chosen because of its low coefficient of thermal expansion and good vibration damping ability.

2. DEFINING DIMENSION USING SIMULATION

As a starting size, the dimensions of the parts were defined, except for the dimensions of the inner granite core. The enclosing dimensions of the aluminum-based bottom and top sheets are taken into account in the simulation tests with values of $552.5 \times 2090 \times 20$ mm.

Due to the right setting, the table is designed with a three-point support system, that allows the right height and leveling to be adjusted perfectly, having a layout which is shown in *Figure 3*. During the optimization of the static stiffness of the structure, these support points will not be changed. Their positions will be adjusted to the appropriate places during the optimization for minimum deflection, caused by the self-weight.

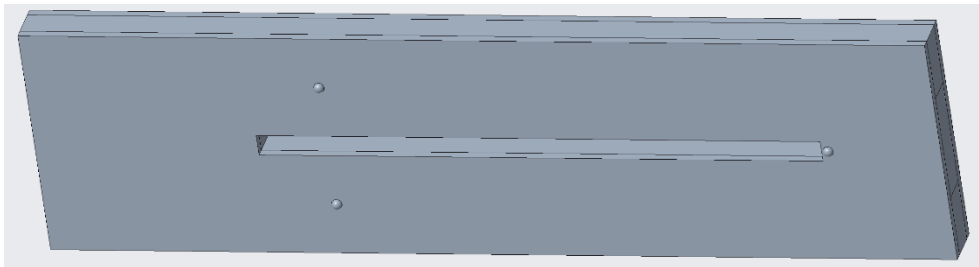


Figure 3. The points of the three-point support system

In order to obtain adequate results in the analyzes, the material properties of each material used must be defined in the software. After entering this data, in the 3D model, the individual parts must be provided with a finite element mesh, and the gluing have to be set on each contact surface, since the assembled table will also be assembled by gluing, these are shown in *Figure 4*.

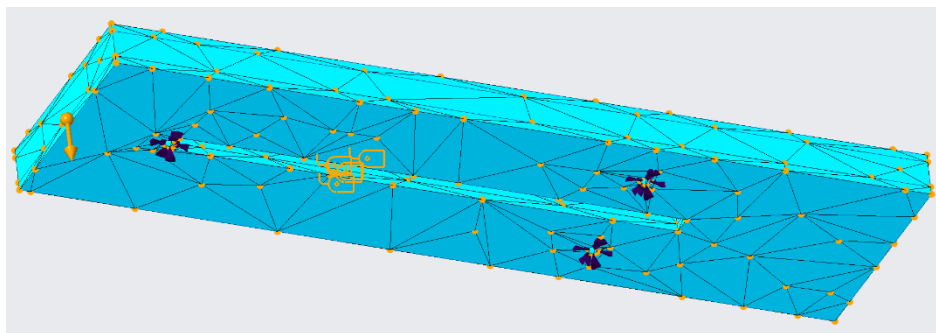


Figure 4. The meshed model with contact definitions

Since the size of the aluminum slabs was fixed at 20 mm, we only changed the geometry of the granite in the middle during the optimization. In doing so, the thickness of the granite block was one variable and the other was the width of the

opening in the granite. Because it is necessary to design the opening on the table, its dimensions will be determined by the aluminum plates, but the dimensions of the filler granite will be different, this is also true for the width of the table. The remaining voids will be filled with polyurethane foam.

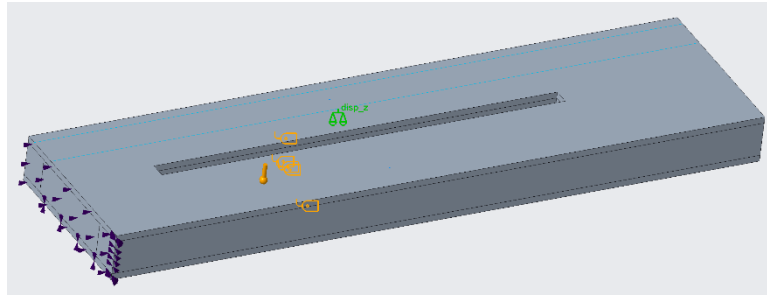


Figure 5. The highlighted point (marked with green)

The opening was examined with several different sizes, the results of these are illustrated in *Figure 6*, in which we examined the displacement of a highlighted point, which is shown in *Figure 5*.

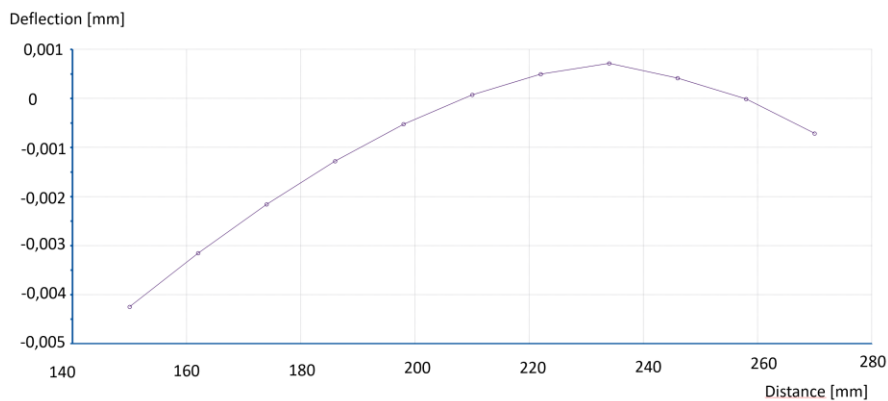


Figure 6

The effect of the opening size on the displacement of the highlighted point

From the simulations it can be concluded that the point displacement is the smallest in the case of opening size around 235 mm, so during further design, we will modify the given elements by keeping this opening close to this value.

3. DEFINING THE DIMENSIONS OF THE THREE-POINT SUPPORTS

To further increase the static stiffness and decrease the deflection of the composite table, the three-point support must be investigated. By choosing its dimensions properly, it is possible to minimize the deflection of the longitudinally asymmetrical

table due to its own weight. For this purpose, various optimization algorithms can be used in engineering design systems to define the variables that we want to bring to an optimal value, and the system determines the value of these variables after the necessary calculations.

Table 1

The definition of the variables during the optimization process

Variable	Current	Minimum	Initial		Maximum	Units
d12:Granit	237	200	210		270	mm
d20:Also	1744	1500	1950		2070	mm
d6:Felso	1617	1500	1950		2070	mm

During the optimization, we wanted to get the longitudinal position of the support points and, depending on them, the thickness of the granite core. To determine the optimal values, the maximum values of the table and the preferred point(s) must be defined (*Table 1*), as a function of which the software determines the geometrical dimensions where the support points and the thickness of the granite give the smallest possible displacement.

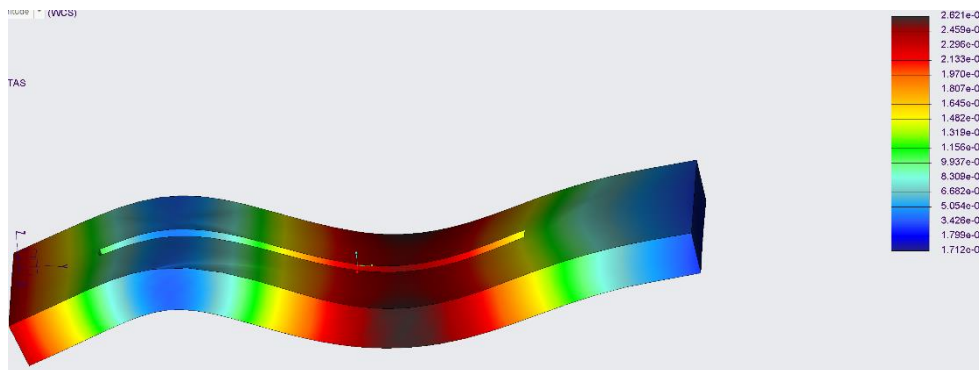


Figure 7. *The result of the optimization*

The obtained results and their mechanical simulation are shown in *Figure 7*. It can be read from the scale that the maximum displacement during the static test is 2.6 μm , which is considered an acceptable value, so the values of the calculated points and the thickness of the granite core are recorded for the further design process.

4. DYNAMICAL ANALYSIS OF THE OPTIMIZED PART

In addition to the static stiffness, the smallest eigenfrequency value of the modified and already statically optimized composite structure have to be determined. Our goal is that the lowest eigenfrequency of the structure exceeds the frequency range that can typically be transferred from the environment to the equipment and cause adverse resonant effects. This range is typically the frequency range of 1 to 150 Hz.

We therefore considered it reasonable to design the structure so that its minimum eigenfrequency falls upwards from the referenced frequency range.

Table 2
The result of the dynamic simulation

Mode	Frequency (Hz)
1	154.23
2	187.48
3	323.11
4	332.05

Based on the data obtained as the result of the calculation (*Table 2*), we can state that the smallest natural frequency of the examined structure is outside the frequency range mentioned. The oscillation image for the lowest eigenfrequency is shown in *Figure 8*. It can be seen from the figure that the first oscillation image (*Figure 8*) typically corresponds to a torsional oscillation around the longitudinal axis.

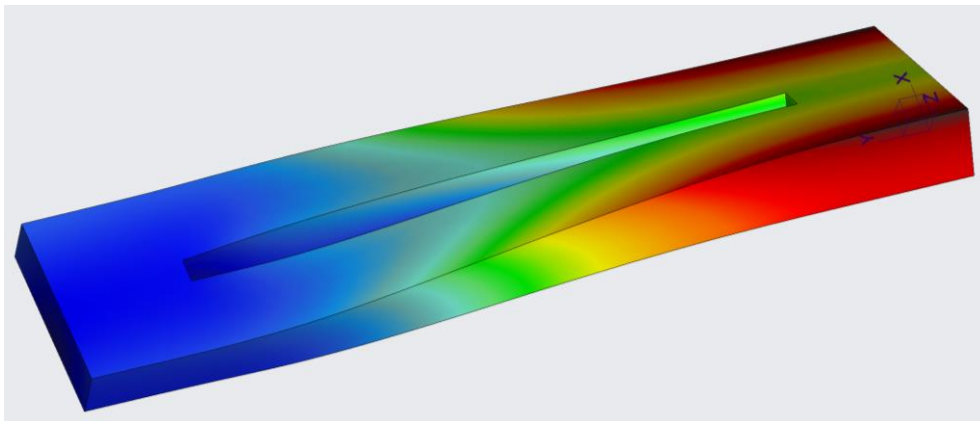


Figure 8. *Oscillation of the first eigenvalue*

5. SUMMARY

In the present article, we have shown how to use numerical methods in the design of an auxiliary table, what we have mainly done with the finite element method. In an example, we demonstrated the necessity and effectiveness of each mechanical test. It has been described how finite element software, which is part of every major engineering design system today, can greatly contribute to the successful completion of engineering work.

ACKNOWLEDGEMENT

The described study was carried out as part of the EFOP-3.6.1-16-00011 *Younger and Renewing University – Innovative Knowledge City – institutional development*

of the University of Miskolc aiming at intelligent specialization project implemented in the framework of the Szechenyi 2020 program. The realization of this project is supported by the European Union, co-financed by the European Social Fund.

REFERENCES

- [1] Baráti, A.: *Szerszámgép-vizsgálatok*. Műszaki Könyvkiadó, Budapest, 1988.
- [2] Páczelt, I.: *Végelelemmódszer a mérnöki gyakorlatban*. I. kötet, Miskolci Egyetemi Kiadó, pp. 36–37.
- [3] Kiss, R. – Szilágyi, A.: Analysis of the dynamic behaviour of the CNC machine centre by FEM. *Design of Machines and Structures*, Vol. 9, No. 1, pp. 24–28, 2019.
- [4] Specifications of Nexus optical tables, https://www.thorlabs.com/newgroup/page9.cfm?objectgroup_id=7139 (2021. 05. 10.).
- [5] Specifications of Hiwin linear Guideways. <https://www.hiwin.it/images/download/documenti/guide-lineari-manuale-assemblaggio.pdf>, pp. 25–26., (2021. 05. 10.).

CASE STUDY: DESIGN OF A VACUUM GRIPPER

DÁNIEL KISS¹ – ATTILA SZILÁGYI²

^{1,2}*University of Miskolc, Department of Machine Tools*
3515 Miskolc-Egyetemváros
¹*kiss.daniel@uni-miskolc.hu*
²*szilagy.attila@uni-miskolc.hu*

Abstract: In this paper we present the design process of a vacuum gripper based on an existing design, which have to be modified. During the design process each step was analysed by finite element methods, to see that the change in the model was made into the right direction. During these steps an appropriate solution was selected to be used later. In the paper we present the base design and the results of its analysis. Later we discuss the modifications made on the model and the final result of simulations of the modified geometries.

Keywords: *FEM, mechanical, numerical*

1. INTRODUCTION

When designing machines, all factors related to the accuracy and in-service parameters of the machine must be taken into account. These factors include deformations and vibrations caused by certain thermodynamic and mechanical phenomena. The effect of these should be taken into account already in the planning phase, since in this case it is the most economical to detect errors. Since the device is not physically available in the design phase, these phenomena can be modelled using simulation software [1].

The part to be examined is a vacuum gripper which have to be modified based on an existing design. The modification is necessary because it have to hold in place bigger pieces, this also means that the structure have to be optimized for minimal deflection caused by the self-weight of the structure [2], [3].

This gripper holds in place different types of foils, during other operations done. The existing design is made for 600 mm wide foils, while there is a demand for holding wider pieces up to around 1,200 mm in width. The paper does not discuss the effect of the vacuum, because that has more effect on the foil rather than on the structure of the gripper.

The material used for this device was selected to be EN-AW 2014-T6 aluminium alloy, which has good mechanical properties, and easy to machine. The design and analyses was done in Autodesk Inventor 2020 design software. This software has a FEM module which can be used for simpler engineering analyses.

2. DEFINING THE MODELS

The assembly of the gripper consists of 4 pieces:

- vacuum plate
- side supports (2pcs)
- middle support

In the beginning simple geometries were made for the support, and vacuum plates, which were modified during the design phase. The initial design is shown in *Figure 1*. In the figure the fixed constraints (white squares) and gravity load (yellow arrow) can be also seen. The middle support only attached to the lower side of the vacuum plate. The notch between the two plates have to be left free accessible. This causes the problem, that the upper side of the plate cannot be supported in the middle which will cause uneven deformation between the two holding plane.

During analysis the automatic mesh generator was used, which uses tetrahedral elements (359,236 elements and 235,247 nodes for the assembly). The element size is defined by a fraction of the bounding box of each part. Since the parts will be assembled by screws, the contact regions were modelled as rigid (bonded) contact. The material definition is the built in properties in the software of the mentioned alloy.

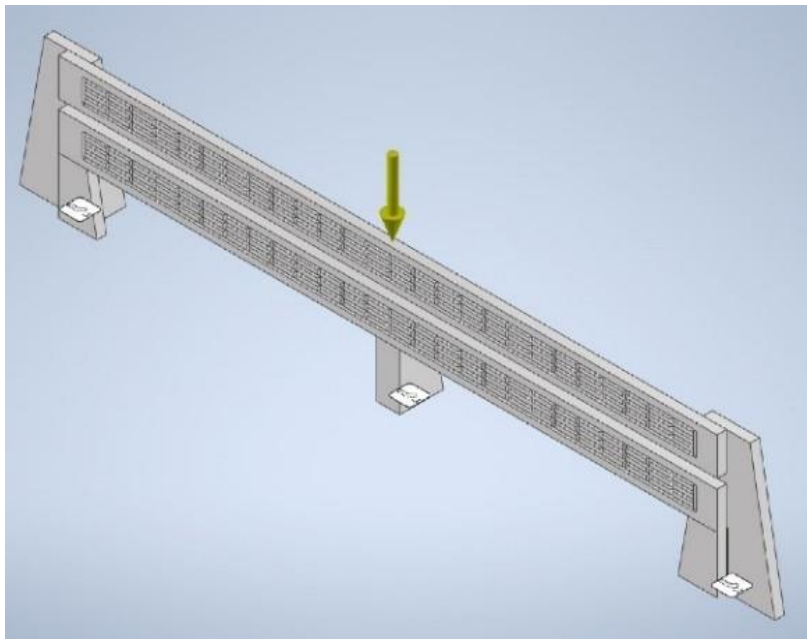


Figure 1. Starting design showing 2 separate vacuum plates, which was later united

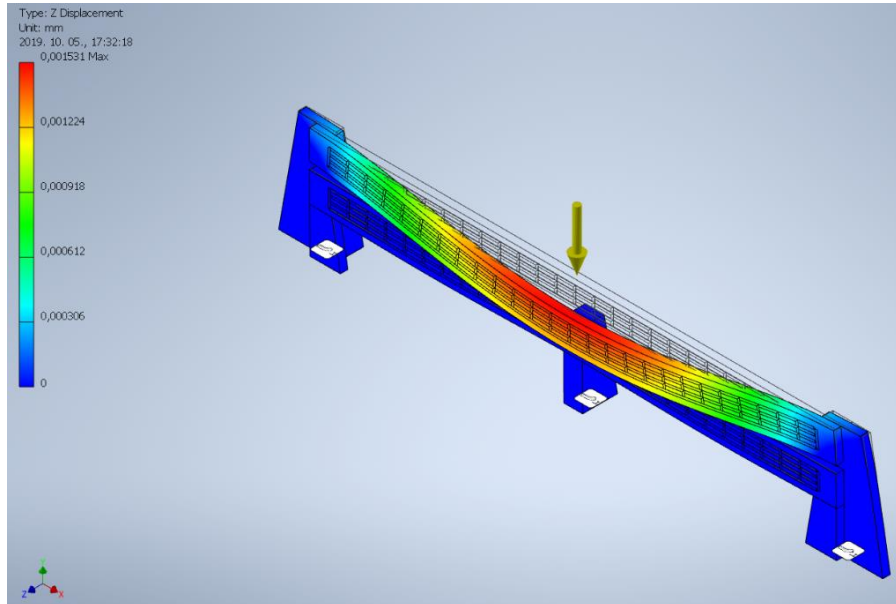


Figure 2. Deflection in transverse direction (Z) (enlarged)

The deflection of the initial model is shown in Figure 2. Buckling can be seen in Z direction, which is inadequate, because it causes the foil also to move off the desired plane. During the next steps these parts have to be optimised to get as low deflections as possible.

Figure 3 shows the cross section of the optimised vacuum plate.



Figure 3. Cross section of the vacuum plate

3. MODIFICATIONS IN THE GEOMETRIES

During the model optimization the support was redesigned first. Since the vacuum plates had to be redesigned also, these modelling steps were interacted to each other. The cross section of the vacuum plates were also redesigned in multiple steps until the optimal solution was found. In conclusion of the performed analyses we can state, that using thicker support, the deflection of the upper plate does not change

significant, therefore an optimal solution was selected, with simple design and reduced weight, which is important for higher eigenvalues of the assembled device.

In *Figure 4* we can see the deflection of the optimized geometry in transversal direction. During several modification in the design, we succeeded to achieve a solution where the transversal deflection is under $1\ \mu\text{m}$. For precise operation of the device this value is adequate.

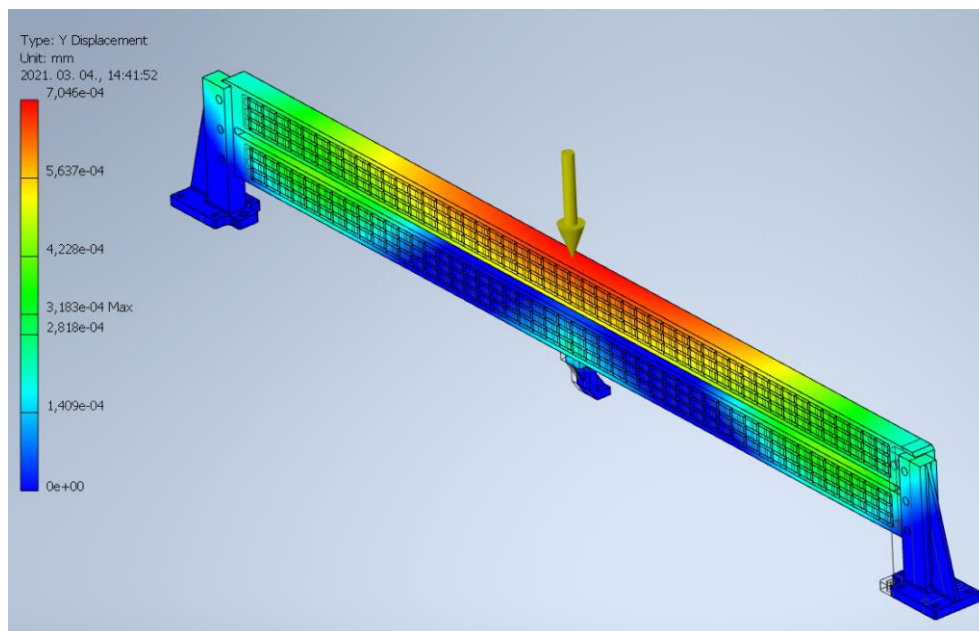


Figure 4. The meshed model with contact definitions

4. DEFINING EIGENVALUES

During operations it is advised to design the device in that way, that the self-frequencies of the device should be over the vibrations that are present from the environment. These frequencies are typically in the range of 1–150 Hz. In addition to the static stiffness, the smallest eigenfrequency value of the modified and already statically optimized structure have to be determined. We therefore considered it reasonable to design the structure so that its minimum eigenfrequency falls upwards from the referenced frequency range.

Table 1

The result of the modal analysis

Mode	Frequency (Hz)
1	88.42
2	188.38
3	217.84
4	274.32

Based on the data obtained as the result of the calculation (*Table 1*), we can state that the smallest natural frequency of the examined structure is only in the frequency range mentioned. Since these parts will be mounted on an optical table, with dampening pads, this natural frequency will not cause deflections and unwanted vibration in the device, because one property of these optical tables and its supports is that these can eliminate unwanted frequencies from the environment with good efficiency.

5. SUMMARY

In the present article, we have depicted the modification of an existing geometry using numerical methods to verify the effects of each modification. We draw the conclusion from the results of the simulations for what have to be modified to get optimised geometry in accordance with the deflection caused by self-weight. The eigenvalues of the structure was also defined, despite the lowest value is in the range of the environmental frequencies, by the usage of other dampening devices, it will not cause any undesired phenomenon.

ACKNOWLEDGEMENT

The described study was carried out as part of the EFOP-3.6.1-16-00011 *Younger and Renewing University – Innovative Knowledge City – institutional development of the University of Miskolc aiming at intelligent specialization* project implemented in the framework of the Szechenyi 2020 program. The realization of this project is supported by the European Union, co-financed by the European Social Fund.

REFERENCES

- [1] Baráti, A.: *Szerszámgép-vizsgálatok*. Műszaki Könyvkiadó, Budapest, 1988.
- [2] Páczelt, I.: *Végeselemmódszer a mérnöki gyakorlatban*. I. kötet, Miskolci Egyetemi Kiadó, pp. 36–37.
- [3] Kiss, R., Szilágyi, A.: Analysis of the dynamic behaviour of the CNC machine centre by FEM. *Design of Machines and Structures*, Vol. 9, No. 1, pp. 24–28, 2019.

ADDITIVE METAL PRINTING MACHINE TOOLS

LOTÁR LÁSZLÓ KISS¹ – GYÖRGY TAKÁCS²

^{1,2}*University of Miskolc, Department of Machine Tools*
3515 Miskolc-Egyetemváros

²*takacs.gyorgy@uni-miskolc.hu*

²*<https://orcid.org/0000-0002-5578-9091>*

Abstract: The 3D printing, as a modern manufacturing method, is becoming more widespread and overrides the usual industry conventions. While it was mainly known in the production of plastic parts, nowadays metal-based versions are also becoming more widespread. Reputable machine tool manufacturers such as DMG Mori or GE compete with each other to create equipment for this technology for the industry, where there is a growing market for such machines. My article seeks to answer the question of where these tools have a place in the industry, whether they can be considered as machine tools, and decide that the procedures describing the construction of machine tools could be applied to them.

Keywords: *metal printing, 3D printing, machine tool, definition, morphology, function block sketch*

1. INTRODUCTION

Metal printing processes, like the plastic versions, can be derived from RPT (rapid prototyping) processes, and these foundations can also be discovered on machines currently used in industry. Although the naming conventions differ from model-to-model, basically most implementations can be treated as a sub-version of DED (direct energy deposition) and PBF (powder bed fusion).

In the case of direct energy deposition, basically the workpiece can be expanded with additional geometries, even with an additional DED head mounted on a CNC cutting machine (hybrid machining). However, in the case of powder bed fusion the entire workpiece is made of metal powder by using a laser's energy to locally melt the powder. Since the latter can be considered as a separate process in itself and as an apparatus, the article is hereinafter limited to this.

2. PRACTICAL APPLICATIONS OF INDUSTRIAL METAL PRINTING

During the research of the metal printing processes, a question may arise that after all do we really need this technology at all. There are countless examples that are hard or impossible to implement with traditional technologies – e.g. the case of cooling ducts running inside the part, the case of parts where most of the material needs to be machined, or a combination of material qualities and complex geometries that are difficult to machine.



Figure 1. 3D printed Ti-Al alloy blades for Boeing power units [5]

A specific example is shown in *Figure 1*, where Boeing forms Ti-Al alloy high-pressure turbine blades with internal cavities and cooling channels. Creating such a geometry from such a material by conventional methods is not profitable and extremely cumbersome.

Figure 2 shows another example that shows that metal printing offers new possibilities in the field of design as well. The two parts offer the same rigidity in terms of load capacity, and it could be seen that the lower version can be made from fractions of the materials used in the machined version.



Figure 2. Possible design of a bracket with machining and 3D printing [6]

The two versions require a completely different design approach, while the first design focus on the simplest possible geometries and then accessibility with machining tools, the second case the viewpoints are the most efficient space filling and connection between the functional surfaces. This provides an opportunity to follow the current trend of weight reduction like in the automotive industry, and make such a relief on the manufactured, which has not been possible so far with conventional methods.

3. THE METAL PRINTING EQUIPMENT AS A MACHINE TOOL

An important and currently controversial question in the industry is, whether or not these machines can be considered as machine tools. To resolve this issue, I use the definition of a machine tool [3].

“A machine tool in the broadest sense is a machine that transforms workpieces with the tools captured in the machine according to the information provided by man, without human effort. According to the material of the workpiece, metal, wood, plastic, etc. machine tools are distinguished.”

The broader definition of the definition can be interpreted without any modification for PBF devices, if the statement is acceptable that the workpiece is the dust and the tool is the laser. By implication, these machines belong to the group of metalworking machine tools.

“In a narrower sense, machine tools for metalworking machines, one of which is machining without chips (presses, hammers, rolling-, bending machines, etc.), the other one is cutting machine tools (lathes, drilling-, milling-, planing-, grinding-, gear-processing machines, etc.). ...

The most important machines in the industry are machine tools because those are only tools that can reproduce themselves, and other machines can be made with them.”

Although there is no specific category for these additive machines in the narrower definition yet, they can be classified as non-chipping machines or should be considered later that change the word “cutting” to “removing or adding material” in the future.

Since the key phrase of the definition is that such a machine should be able to reproduce itself, which is maximally fulfilled for these machines, I will consider PBF metal printing machines as machine tools in the rest of the article.

4. CONSTRUCTION CONSTRAINTS AND FEATURES

Before starting the analysis, it is generally worth looking at the constraints and features of PBF metal printing machine tools, which will be aided by *Figure 3* (<https://en.dmgmori.com/products/machines/additive-manufacturing/powder-bed/lasertec-30-slm>).

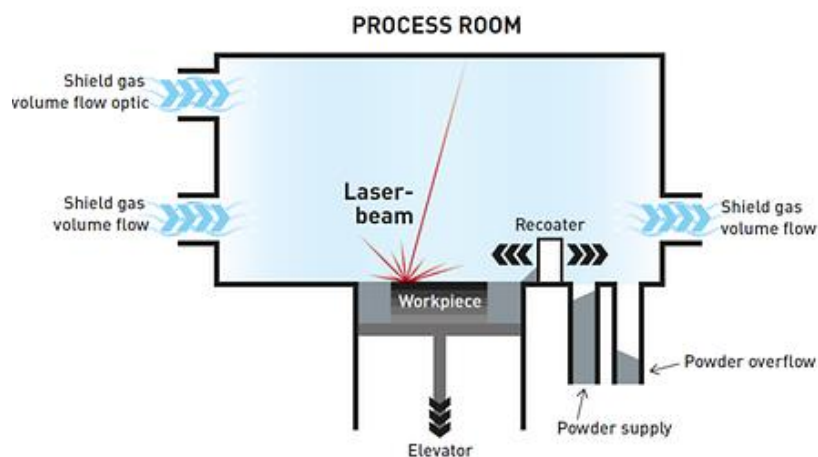


Figure 3. Additive manufacturing by selective laser melting (SLM) in powder bed

After spreading the powder layer, the entire cross-section of the workpiece is created with a laser beam, and then the process is repeated after the table has sunk. Examining the operation of the procedure, the following constraints can be identified:

1. The easiest way to spread the dust is done by gravity, the table must be placed in a horizontal position at the bottom.
2. The laser must be located on the opposite side of the powder bed so that it will work from above.
3. The laser should be able to cover the entire work area while it should not fall under a critical angle ($\sim 45^\circ$), because in this case it will more likely melt sideways rather than downwards.
4. The shielding gas supply should be laminar to not stir up the dust from the bed.

This is a surprising amount of constraint compared to a CNC cutting machine, but it will be seen later that there will still be a lot of options in the moving of the laser.

Before examining the features, it is worthwhile to find out the definition of the D-number based on the source [3], to find out, how it can be interpreted in such a case.

“D-number for machine tools with serial kinematics:

The number of components in the forming mechanism that are capable of performing some elemental transformation (displacement or rotation) independently and simultaneously to create relative motion between the tool and the workpiece.”

According to this definition, since only stand-alone and simultaneous motion implementations have to be considered, PBF machine tools are 2D (or can be called 2.5D according to industry conventions), since moving the table is not simultaneous with moving the laser, and it only plays a positioning, stepping role. It also could be seen that the movement of the table, cannot be replaced by the up and down movement of the laser, as it is necessary for dust spreading by the recoater.

Previously, in reinterpreting the definition of a machine tool, an analogy was established that the laser is the tool and the dust is the workpiece. It follows from this statement that the vertical axis is perpendicular to the powder table, pointing outwards from the laser, will be the Z + axis of the machine tool, and the other axes will be chosen to form a right-handed coordinate system accordingly.

5. POSSIBLE MACHINE TOOL STRUCTURES BASED ON MOTION SHARING AND ORDER

Although the constraints do not specify the construction kind of the kinematic chain of the machine, but serial kinematic solutions will be taken into account below as they have better workspace coverage. The machine tool structures that can be implemented on the basis of motion sharing and order, considering the constraints and features, are shown in *Table 1*.

Table 1
Possible second-order machine tool structures

	First-order solutions	Second-order solutions
1.	X(m), Y(m)	X(m,1), Y(m,2)
2.		X(m,2), Y(m,1)
3.	X(m), Y(s)	X(m,1), Y(s,1)
4.	X(s), Y(m)	X(s,1), Y(m,1)
5.	X(s), Y(s)	X(s,1), Y(s,2)
6.		X(s,2), Y(s,1)

Analyzing the variations, there are two options – moving the powder table or the laser sideways. In the first case, it should be kept in mind that the powder table can weigh tons if it is completely filled with powder, which is therefore difficult to move precisely.

In the case of moving the laser, mirrors can be considered, as well as moving the laser itself – in the first case, the protection of optical devices becomes a challenge, while in the second case, in addition to protection, there is also a risk of breaking power cables.

Considering the precision requirements for these machines and the serious movement challenge that the dust table would pose, it is much easier to move the laser beam with adequate protection it identifiable that PBF machine tools are recommended to be designed so that it is superimposed to the tool.

6. COMPARATIVE STUDY OF THE MAIN COMPONENTS OF THE PBF PRINTER

Like cutting machine tools, PBF machine tools used in industry are made up of commercial or custom-made components. In many cases the components, in terms of their function and location, are comparable to the units used in cutting machines. The components to be compared are shown in *Table 2*.

Table 2
Machine tool components to be compared

Cutting machine tools	PBF machine tools
Spindle-motor	Laser
Cooling and lubrication system	Shielding gas system
Chip management system	Dust management system
Covers	
Slide rail systems	
Workpiece-switching system	Dust-removal system
Stands, holders	
Tool-switching system	–
	Recoater

For the study, the so-called function block diagrams have been prepared (their format is included in the source [3]), which show in a clear graphic format what functions the components have to implement and provide comparability between different solutions.

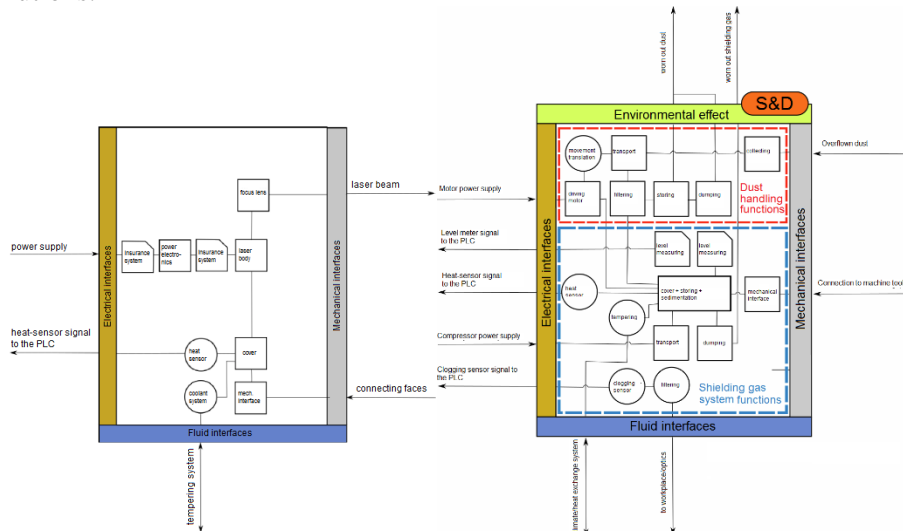


Figure 4. Function block diagram of laser (left) and shielding gas/dust treatment (right) [5]

As an example, *Figure 4* shows a schematic of the function block of the laser and shielding gas and dust treatment subsystem. Based on the figures of the cutting machines using the source [3], it can be seen that there are serious differences in the laser-spindle motor relation, while in the other case there are also serious similarities.

7. SPECIFIC IMPLEMENTATIONS OF SOME MANUFACTURERS

Reviewing the current industrial implementations available on the market, it can be stated that the previous findings of the article are applicable when examining them as well. Concepts such as workspace, machining accuracy can also be defined for these machines, and the components and features described earlier can also be found.

By summarizing the machines into a voluminous knowledge matrix [4], it is possible to determine the average parameters of the machine tools currently on the market. These can be used later for further design tasks. Examples of such values are the $350 \times 350 \times 350$ mm workspace size or the ± 0.03 mm positioning accuracy, which can be fitted to most of the machines.

8. SUMMARY

The first half of the article described the modern additive metal printing processes and their possibilities and their prevalence in industry. By reinterpreting the defini-

tion of machine tools, it can be concluded that these machines can indeed be considered as machine tools, and in support of this, it has been described how the machine tool morphology and function block diagrams can be used to examine these modern machine tools. By counting the equipment currently available on the market in a knowledge matrix, it has become possible to determine average parameters, which together with the function block diagrams can provide a basis for the design of PBF metal printing machine tools.

REFERENCES

- [1] Duda, T. – Raghavan, L. V.: 3D metal printing technology: the need to reinvent design practice. *AI & Society*, Vol. 33, Nr. 2, 2018, pp. 241–252, DOI: 10.1007/s00146-018-0809-9
- [2] Mohammed Ali, S. – Bäckström, C.: *Present and future of Additive Manufacturing*. Master's thesis, 2020, University of Karlstadt
- [3] Takács, Gy. – Szilágyi, A. – Demeter, P. – Barak, A.: *Forgácsoló szerszámgépek*. Nemzeti Tankönyvkiadó, 2009.
- [4] Kiss L.: *Additív fémnyomtató szerszámgépek*. TDK-dolgozat, Miskolc, 2020.
- [5] GE: *Blades and Bones: The Many Faces of 3D Printing*. 2013, www.ge.com.
- [6] GE: *3D-Printed 'Bionic' Parts Could Revolutionize Aerospace Design*. 2017, www.ge.com

DESIGNING A FILAMENT RECYCLING EXTRUDER

BARBARA KMETZ¹ – ÁGNES TAKÁCS²

^{1,2}*University of Miskolc, Department of Machine and Product Design
3515 Miskolc-Egyetemváros
¹kmetzbarbara@gmail.com; ²takacs.agnes@uni-miskolc.hu
²<https://orcid.org/0000-0002-3210-6964>*

Abstract: In this paper we can read about designing and building a filament recycling machine especially designed for 3D printers. 3D printing is quite popular nowadays, but unfortunately the base material of this technique is polymer, which is not an environmentally friendly material, but it can be recycled in most of the cases. The filament pieces are shredded beforehand with a shredding machine to get the appropriate size. After being chopped up and heated up to the given temperature, according to the materials specific parameters the filament can be melted down and extruded again. The study deals with designing a recycling machine as mentioned.

Keywords: 3D printing, recycling, filament, extruder, PID, Solid Edge

1. INTRODUCTION

The structure of the machine is shown in *Figure 1*. The extruder consists of many elements as a result it needs coordinated designing.

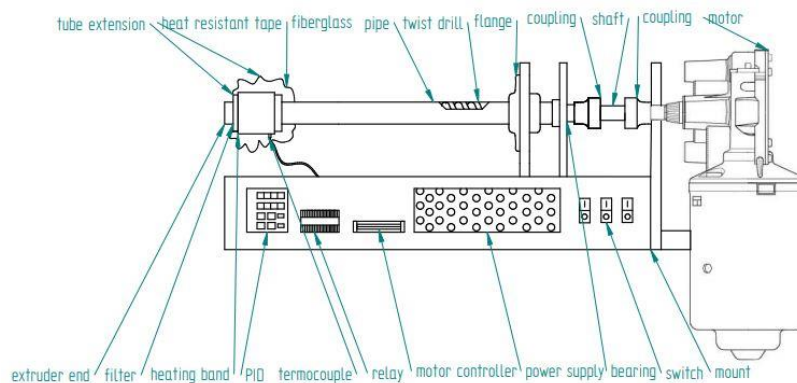


Figure 1. Sketch of extruder machine

The extruder unit contains two main parts. One is the user interface and the other one is the machine's workspace. The user interface displays the control buttons of different units. By pressing the buttons, the motor can be started, the ventilator can

be activated, the heating can start and with the potentiometer the motor's speed can be adjusted. The setup of the extruder is far more complicated. The rotation movement is granted by a simple windshield motor, which is forwarded by a shaft coupling. The compressive force is wiped out by an axial roller bearing and the next element in the shaft line is a twist drill. The twist drill is responsible for forwarding the filament pieces. The end of the twist drill can be heated to the desired temperature by a brass band. The twist drill is covered by a tube from the outside. The heating band must be insulated well to keep the warm better, the applied fiberglass and the different types of heat resistant tapes serve this purpose. The heated and melted material leaves the end of the extruder and is winded into a coil.

2. EXTRUDER MOVING UNIT

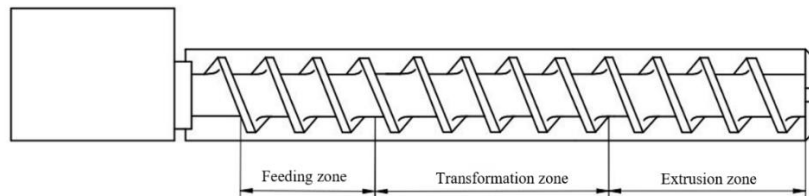


Figure 2. Extruder zones

During the designing process of the extruder, first the size of the extruder was determined first, and the other parts were designed accordingly. The efficiency of the motor and the sustainment were also calculated according to the mentioned units. The studied researches show that the size of the twist drill must be determined first. It is chosen according to the type and size of the material we have to use for the extrusion. [1], [2] The size of the twist drill is 16 mm (M16). This is resulted as the filament pieces are a maximum of 5 mm. According to the references the diameter of the twist drill and the length of the extruder tube should be according to the following rate [3].

2.1. The length of the extruder and extruder tube

The extruder's size must be considered, and the length must be chosen according to the found literature. These rates are the following:

- Extruder's length: $D = 16 \text{ mm}$
- Extruder tube length: $L = 200 \text{ mm}$

The rate of the extruder and the extruder tube:

$$d \div L \tag{1.1}$$

Examples for standard extruder-tube rate length:

1: 10; 1: 12; 1: 12.5; 1: 14; 1: 15; 1: 16; 1: 18; 1: 20; 1: 22.5; 1: 25

Calculated extruder-extruder tube rate:

$$d \div L \rightarrow 16:200 \rightarrow 1:12.5 \quad (1.2)$$

The chosen standard rate is 12.5.

The exact final length is determined during the designing process of the structure.

The extruder can fit in the 18 mm outer diameter tube precisely, the wall of the tube is not too close nor too far from the twist drill. This is a key part of consistent extruding. The extruder tube is designed to be 200 mm long. The 200 mm long element was chosen consciously as the structure required this size for the element. From the extruder and the extruder tube it is given that with the help of the twist drill geometry, the solid flow rate can be calculated and estimated. The next chapter describes the calculation process which refers to the flow rate of the extruder feeding zone.

2.2. Solid state flow rate

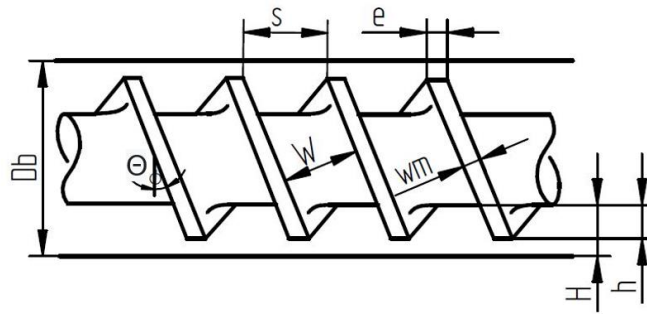


Figure 3. Extruder geometry

The given geometry helps in the calculating process as the following elements measures are known and can be used for calculations. [4]:

- Tube diameter: $D_b = 17 \text{ mm} = 0.017 \text{ m}$
- Screw thread: $s = 12 \text{ mm} = 0.012 \text{ m}$
- Thread number: $\nu = 1$
- Thread width: $w_m = 10 \text{ mm} = 0.01 \text{ m}$
- Channel between the threads: $W = 15 \text{ mm} = 0.015 \text{ m}$
- Depth of feeding zone in the tube: $H = 6.5 \text{ mm} = 0.0065 \text{ m}$
- PLA transport efficiency: $h_{F,PLA} = 0.395$
ABS transport efficiency: $h_{F,ABS} = 0.235$
- Speed of twist drill: $N = 50 \text{ rpm} = 50 \text{ 1/min} = 3000 \text{ 1/h}$

- Bulk density of polymer: $\rho_{0,PLA} = 1.24 \text{ g/cm}^3$

$$\rho_{0,PLA} = 1,240 \text{ kg/m}^3$$

$$\rho_{0,ABS} = 1.06 \text{ g/cm}^3$$

$$\rho_{0,ABS} = 1,060 \text{ kg/m}^3$$

- Solid state rate flow calculation and solution:

$$\dot{m} = 60 \cdot \rho_{0,PLA, ABS} \cdot N \cdot h_F \cdot \pi^2 \cdot H \cdot D_b \cdot (D_b - H) \cdot \frac{W}{W+w_m} \cdot \sin\theta \cdot \cos\theta \quad (2.1)$$

- Calculation of Θ helix angle:

$$\theta = 30^\circ = 30^\circ \cdot \frac{\pi}{180} = 0.5235987756 \text{ rad} \quad (2.2)$$

- Solid state flow rate calculation for the two materials:

$$\dot{m} = 60 \cdot \rho_{0,PLA} \cdot N \cdot h_F \cdot \pi^2 \cdot H \cdot D_b \cdot (D_b - H) \cdot \frac{W}{W+w_m} \cdot \sin\theta \cdot \cos\theta \quad (2.3)$$

$$\dot{m} = 60 \cdot 1,240 \frac{\text{kg}}{\text{m}^3} \cdot 32 \frac{1}{\text{min}} \cdot 0.395 \cdot \pi^2 \cdot 0.0065 \text{ m} \cdot 0.017 \text{ m} \cdot (0.017 - 0.0065 \text{ m}) \cdot \frac{0.015 \text{ m}}{0.015 \text{ m} \cdot 0.01 \text{ m}} \cdot \sin(30^\circ) \cdot \cos(30^\circ) = 463.06 \frac{\text{kg}}{\text{h}} \quad (2.4)$$

$$\dot{m} = 60 \cdot \rho_{0,ABS} \cdot N \cdot h_F \cdot \pi^2 \cdot H \cdot D_b \cdot (D_b - H) \cdot \frac{W}{W+w_m} \cdot \sin\theta \cdot \cos\theta \quad (2.5)$$

$$\dot{m} = 60 \cdot 1,060 \frac{\text{kg}}{\text{m}^3} \cdot 32 \frac{1}{\text{min}} \cdot 0.395 \cdot \pi^2 \cdot 0.0065 \text{ m} \cdot 0.017 \text{ m} \cdot (0.017 - 0.0065 \text{ m}) \cdot \frac{0.015 \text{ m}}{0.015 \text{ m} \cdot 0.01 \text{ m}} \cdot \sin(30^\circ) \cdot \cos(30^\circ) = 395.8439 \frac{\text{kg}}{\text{h}} \quad (2.6)$$

The calculated values consider the full cross section of the tube (226.98 mm²) in relation to possible amount of solid flow rate. The actual considered trans section is much smaller than the one used in the calculations; this means that the solid flow rate would also be smaller. The examined new cross section is approximately 0.01767 mm². With the use of this new section we got the following calculations. The solid flow rate of PLA would be approximately 18.5732 kg/h and the solid flow rate of acrylonitrile butadiene styrene would be approximately 15.8457 kg/h according to the pre-planning phase of the designing. The two materials distribute similar characteristics, (like density) that is why the two materials' calculations are close to each other. These calculations can help to estimate the amount of filament the recycling machine will be able to extrude in an hour [5]. In practice the flow rate will reduce to a lot less to the fragment of the calculated numbers because of the heating, melting and the cooling process.

The considered area is the useful area according to the shredded material because the materials arrival happens through this cross section. This area should be connected to the shredders bottom. The connection is created by a dispenser element. The dispenser was designed in Solid Edge and it was 3D printed from PLA because it does not have to withstand great temperatures.

The twist drill is longer than the tube and it continuous to the engine in a square shaft part. The end of the extruder and the motor is connected by a coupling element. One end of the coupling fits the extruder, also the other end fits the engine shaft. In the current situation a single square iron part was the coupling element. While choosing the right motor for the machine, some references and similar literatures were considered. As these papers also suggested a simple windshield motor was chosen to be the heart of the recycling machine. (medium.com) (www.filastruder.com).

The structure needs a solid base to stand on with all its elements to keep the machine steady and solid. This base was chosen to be a Hilti mounting rail which was an obvious because of its modular function. The structure also has a holding element, which fixes the extruder tube and the motor shaft. The end of the tube has an axial roller bearing on it. This bearing helps in cancelling out the compressive force coming from the kickback. The kickback protection is important for the motor because it is not designed to endure this kind of load, but to rotate. Because of this condition it is appropriate to examine the bearing force and the bearing lifetime estimation.

3. HEATING PANEL

The design and assembly of the heating panel is the most complicated part of the structure, because it contains not only mechanical components but electronic parts also which need special attention and calculation. Electric parts need to be synchronized which can be quite hard if someone does not have the electrical skills to execute it. It is easier to understand the methodology of the heating panel if we look at the elements after one another. The tube with the 18 mm outer diameter is lengthened by a brass element which has better heat conductivity than stainless steel. This section will be heated for the desired temperature, as a result a brass heating band is placed on the 50 mm lengthened brass part. (edge.rit.edu) (www.printfromsd3d.com) The heating band is responsible for getting the temperature displayed on the PID, with the help of the K thermocouple sensor. The thermocouple is the actual part sensing the temperature and the PID is adjusting according to its measures. The thermocouple is placed in the brass tube lengthening in a 3 mm hole causing it to show the exact temperature the machine has in the extruder zone. After the brass tube only one element is left from the machine, this one is the extruder end which closes the system and the melted filament is heading out from its hole to cool down.

4. ELECTRONIC PANEL

This chapter is about synchronizing and connecting the different electric elements. Every electrical part is somehow connected to the power supply this is why the right

power supply should be chosen considerably. Considering all the elements the power supply must be a little bit more powerful than expected not to cause any short circuits. The chosen power supply is operating at 12 V, with 240 W output and 20 A current.

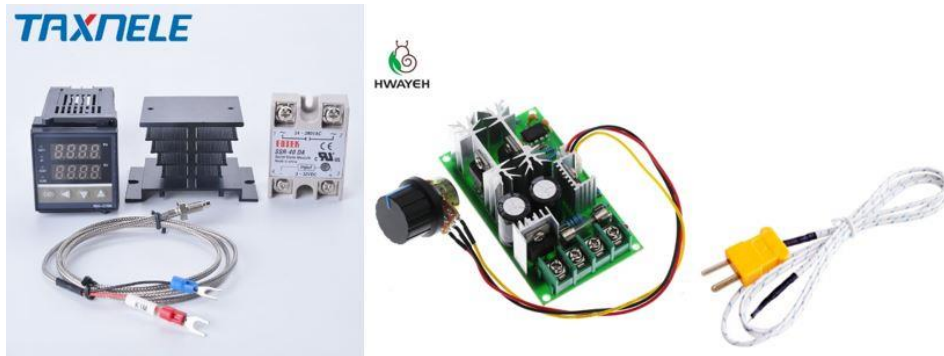


Figure 4. PID, motor controller, K thermocouple

The three buttons will start the whole machine's operation, one of these gives power to the machine, the other one starts the motor, the third one starts the ventilator. The user interface also has a potentiometer attached to it; this serves the ability to control the motor's speed. The motor gets power through the controller. The ventilator connected to the machine is responsible for cooling the filament which comes out of the extruder end. The PID also receives power from the power supply and is connected to the mentioned K thermocouple and the heating band. The heating band has 220 V stress, but the PID operates only at 12 V, therefore the electric panel needs a solid-state relay to connect the two elements. The ground port and the 220 V of the power supply are connected to the other two pots of the solid-state relay. When the relay closes, the heating band is heated according to the PID's signal and when the relay is open the signal will not reach the heating band and it will not heat up. The electric control works as it is described in this chapter.



Figure 5. Extruder model and machine

5. SUMMARY

The research reflected on designing the element and the structure of a machine. The required calculations were executed and considered as the measurements were established. The length rate and the solid flow rate was calculated. The heating panel and the electronics were described in details and the model and the building of the structure was introduced in the article. The result of the study is a working extruder machine with a user-friendly interface ready for testing.

ACKNOWLEDGEMENT

Supported by the ÚNKP-19-2 New National Excellence Program of the Ministry for Innovation and Technology.



REFERENCES

- [1] Michaeli, W.: *Extrusion Dies for Plastics and Rubber*. Hanser Publisher, Germany, 1992, ISBN 3446161902.
- [2] Lafleur, P. – Vergnes, B.: *Polymer Extrusion*. ISTE Ltd. and John Wiley & Sons, Inc., USA, Great Britain, 2014, ISBN 9781848216501.
- [3] Wagner, J. – Mount, E. – Giles, H.: *Extrusion: The Definitive Processing Guide and Handbook*. Elsevier, Inc., USA, 2014, ISBN 9781437734812.
- [4] Birley, A. – Haworth B. – Batchelor, J.: *Physics of Plastics Processing, Properties and Materials Engineering*. Chapter 4., Hanser Publisher, Munich, Cincinatti, 1992.
- [5] Rao, N. – Schott, N.: *Understanding Plastics Engineering Calculations*. pp. 67–70, Hanser Publisher, Munich, Cincinatti, 2012, ISBN 9781569905098.

STEPS OF GENERATIVE DESIGN IN INTEGRATED CAD SYSTEMS

KRISTÓF SZABÓ

*University of Miskolc, Department of Machine Tools
3515 Miskolc-Egyetemváros
szabo.kristof@uni-miskolc.hu*

Abstract: Due to the continuous development of various areas of the industry, such as modern production equipment, material technology, computer and software development, it is possible to expand the range of conventional production technologies. These include additive manufacturing technology, which provides a new opportunity to produce everyday products, thereby satisfying market needs. Integrated CAD systems have occupied a place in the product design and development process for decades, which has partially reformed classical design methods and its steps.

Keywords: *product design methodology, topology optimisation, generative design*

1. INTRODUCTION

A successful product meets the level of technical development of a given period and fulfils the needs expressed by society. The aim of engineering design is to create a suitable solution for a given problem, both from a technical and economic point of view. Product design and development is an outstanding and special profession, as it requires extensive experience, a unique vision and additional specific skills. Earlier it has been accepted that the knowledge required for successful product design is a talent that cannot be fully learnt, described, is not an exact science, and cannot be mechanized. It was recognized in a short time that the quality of a product is greatly influenced by the concept defined and selected in the design phase. Furthermore, a series of decisions that arise during the design procedure play a key role in the product manufacturing process, which can result in beneficial or disadvantageous changes. Based on this philosophy, it can be said that in terms of the life cycle of a product, innovation activities consume huge resources. Assuming that this type of activity can only be properly performed by a competent person, design and development work proves to be an expensive and long procedure. The increasing expectations dictated by the market can be met as much as possible if a given product can be sold as soon as possible and with the lowest financial cost. Accordingly, the design and construction tasks must be transformed into tasks that can be performed by many, in which the individual stages and steps can be well followed and performed [1].

2. MILESTONES OF DEVELOPMENT OF DESIGN METHODOLOGY

The development of various design methodological processes could be observed in the last hundred years. Literature related to the field can be found mainly in Europe, but there are researchers from all over the world whose work is related to this field of science. The aim of the research is unchanged: the design process must be divided into different stages, which can be clearly interpreted and followed in order to be applicable for others. Kesselring published on evaluation procedures as early as 1937 and then presented the basics of his convergent approximation procedure. Wögerbauer proposed in 1943 that the entire design process should be divided into subtasks. The founders of the Ilmenau school were Bischoff and Hansen. Hansen has been working on the basics of design methodology since the 1950s, and, in 1965 he summarized the theoretical aspects of his system. The founder of the Berlin school is Beitz, whose work is closely linked to the founder of the Darmstadt School of Design, Pahl. In 1974, Roth was among the firsts to realize that methodical design could be successfully automated using graphics computers and then developed an algorithmic design model. In Hungary, the Budapest School of Design is worth mentioning, which deals with the development and research of product design methodology and tools. The Hungarian founder of this topic is Bercsey, who developed the Autogenetic Algorithm. It is important to mention the design school in Miskolc, which was founded by Terplán and Tajnafői, and computer structure generation methods were created by Lipóth and Takács [2], [3].

3. GENERATIVE DESIGN AND INTEGRATED CAD SYSTEMS

The generative design model is able to generate concepts using predefined requirements and constraints. The procedure, including shape and topological optimization, was developed around the 1990s, but at that time could not lead to breakthrough success.

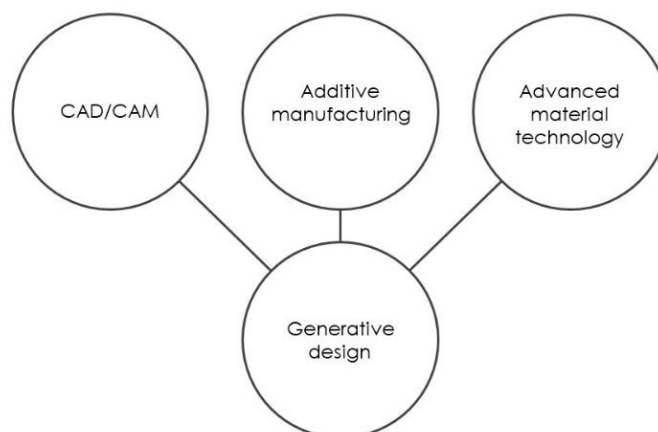


Figure 1. The technological need of generative design

The use of the programs was cumbersome, the capacity of the computers proved to be insufficient, but the main drawback was that the result obtained could not be produced with the help of the traditional manufacturing technologies of the given era. Over the next 20 years, the production of additives provided an opportunity to implement 3D printing, and in the early 2000s it became clear that there was an opportunity for additive production of high-performance metallic components, which attracted interest among integrated software manufacturers. Software supporting generative design appeared in the first half of the 2010s. Among the firsts TrueSOLIDTM from Frustum can be mentioned, developed by Jesse Coors-Blankenship. The other big developer is Autodesk, but recognizing the need for generative design, more and more software development products have become available, which are summarized in *Table 1*.

Table 1
Generative design softwares

	Software developer	Product
Generative design software	Frustum	Generate
	nTopology	Element
	Paramatters	CogniCAD
CAE software supporting generative design	Altair	OptiStruct
	ANSYS	ANSYS Mechanical
	Dassault Systèmes	Tosca Structure, Tosca Fluid
	ESI Group	PAM-STAMP, ProCAST, SYSTUS
	MSC Software	MSC Nastran Optimization
Integrated systems with generative design module	Autodesk	Fusion 360, Inventor
	Dassault Systèmes	TOSCA suite
	Robert McNeel & Associates	Rhino
	PTC	Creo Simulate
	Siemens	NX, Solid Edge
	Altair	solidThinking Inspire

4. STEPS OF GENERATIVE DESIGN IN INTEGRATED CAD SYSTEMS

Generative design is a design process in which an algorithm is used to optimize the shape of a part for a given boundary condition. Designing the shape itself is not a manual design task. The designer determines the functional boundary conditions of the part, adds it into the software, which calculates the shape of the optimized part according to the defined aspects during iteration processes [4], [8]. Limit states can usually be divided into two groups, the calculation requires an initial geometry,

which must be constructed by traditional 3D modelling. This is quite similar to the solution used in traditional FEM systems: it is necessary to determine which area of the piece is subjected to which forces and which constraints [5–7]. Another possibility is to determine the volumes in which there can be no material because, for example, some other component is moving there. If there is no starting workpiece, it should be specified as a “volume part” that will be part of the finished part. The steps in the generative design process that are valid and show similarity using all the integrated CAD systems listed in *Table 1* are detailed below.

After opening the given program, our first step is to define the design volume, for which we have three options. The first way to do this is to define the geometries to be retained, which remain an integral part of the yellow geometry. Specifying them is a mandatory operation, and later these bodies and surfaces allow defining functions, such as placing mortises. The second method of design space is to define so-called interfering geometries, which can be used to specify those parts of space where there can be no material. The geometry produced by the program can only be located outside this space, but it can be applied in a similar way when the part is limited in size. These volumes are optional during design. The third method is to import a solid-state model whose shape features can be used to specify functions. In this case, the outer surface of the original model does not limit the enclosing size of the geometry produced during generative design by default.

After the precise definition of the design space, the second stage of the process can follow, during which the fixing points and further constraints of our model can be defined. It is possible to specify fixed points, but it is possible to unlock individual planes and axes of rotation within it. We have the option of creating a hinge or pivot point where radial, axial and tangential movement can be allowed. Furthermore, it is allowed to define slip planes and friction surface pairs.

In the third stage of design, we get to defining the location and magnitude of the loads. We have the ability to accommodate force, pressure, torque and distributed load, the direction and magnitude of which can be changed indefinitely.

The fourth step is to decide on the design criteria and objectives. This can be minimizing mass, maximizing stiffness, or developing minimal stress and its optimal distribution. In this phase, a so-called safety factor can be set.

In the fifth step, it is possible to choose the production method, where the production volume and the appropriate production technology can be selected. Optional technologies include additive manufacturing, cutting processes such as milling, cutting and casting. For each option, the minimum material thickness for the model and the tools used in the particular technology, such as the geometric size of the milling tool and the machining direction can be chosen. There is also the possibility that this step will remain unselected, in which case the generation of models will be more widely allowed.

In the sixth step of the process, the material has to be chosen from which the product can be made. The selection can be made from the material catalogues of the programs, but a new material with unique properties can also be defined. The material properties of the items in the catalogue can be modified without any problem.

Care must be taken to ensure that each manufacturing technology has a set of compatible materials.

After making these settings, a verification step becomes available that runs through the data we enter and alerts the user in case of lack of data or poorly entered conditions.

Once the check is done, the planning, i.e. the final calculation and generation process, can be started. We have the opportunity to filter the obtained solutions by categories and access the iteration results of the individual components.

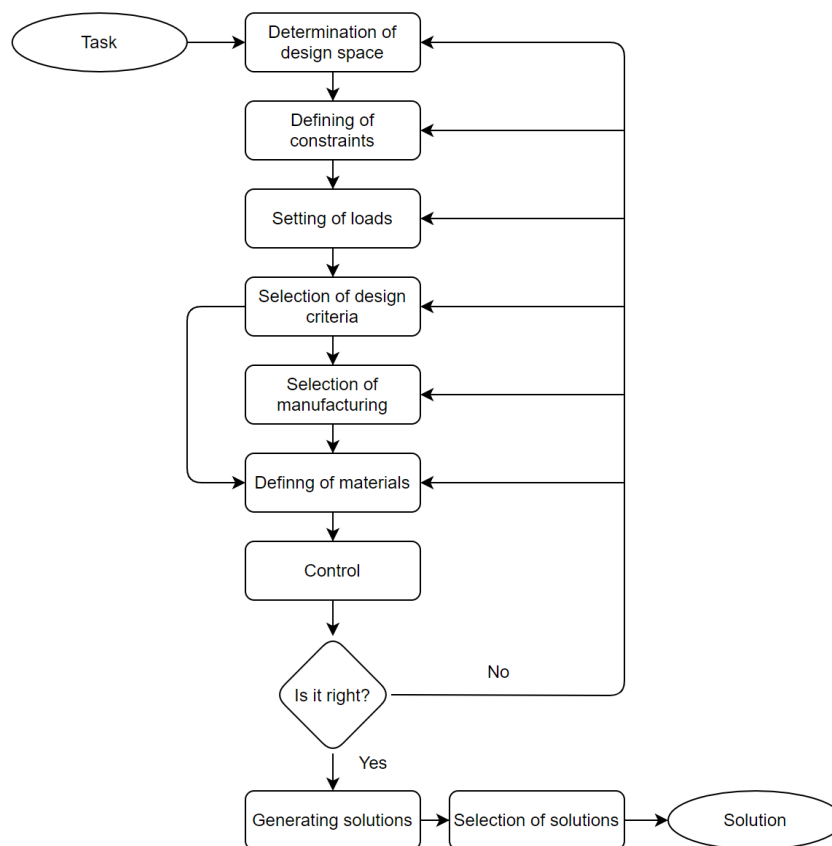


Figure 2. Steps of generative design process

5. SUMMARY

The article reviews the development of the product design- and development field that forms the basis of generative design, as well as its defining stages. Factors influencing the spread of the generative design process and the development of the necessary technological processes are presented, and the article provides a short historical overview of the topic of software supporting. Based on the software listed, the article describes

the steps required to use the method, which show a match for different programs. For quick understanding and illustration, a flowchart for the operation of the method was created, supplementing the possible iterations. By observing and following the steps properly, we get successful solutions to the formulated task.

ACKNOWLEDGEMENT

The described article/presentation/study was carried out as part of the EFOP-3.6.1-16-00011 *Younger and Renewing University – Innovative Knowledge City – institutional development of the University of Miskolc aiming at intelligent specialisation* project implemented in the framework of the Szechenyi 2020 program. The realization of this project is supported by the European Union, co-financed by the European Social Fund.

REFERENCES

- [1] Takács, Gy. – Zsiga, Z. – Szabóné Makó, I. – Hegedűs, Gy.: *Gyártóeszközök módszeres tervezése*. Nemzeti Tankönyvkiadó, Miskolc, 2011.
- [2] Kamondi, L. – Sarka, F. – Takács, Á.: *Fejlesztés-módszertani ismeretek*. Nemzeti Tankönyvkiadó, Miskolc, 2011.
- [3] Takács, Á.: Computer Aided Concept Building. *Solid State Phenomena*, Vol. 261, 2017., pp. 204–207, DOI: 10.4028/www.scientific.net/SSP.261.402.
- [4] Szabó, K. – Hegedűs, Gy.: A generatív tervezést támogató szoftverek rövid áttekintése. *Multidiszciplináris Tudományok*, Vol. 10, No. 3, 2020, pp. 328–337, DOI: 10.35925/j.multi.2020.3.39.
- [5] Zuo, K. – Chen, L. – Zhang, Y. – Yang, J.: Study of key algorithms in topology optimization. *International Journal of Advanced Manufacturing Technology*, Vol. 32, No. 7–8, 2007, pp. 787–796, DOI: 10.1007/s00170-005-0387-0.
- [6] Bendsoe, M.: *Optimization of Structural Topology, Shape and Material*. Springer Verlag, Berlin, 1995., DOI: 10.1007/978-3-662-03115-5.
- [7] Rozvany, G.: Aims, scope, methods, history and unified terminology of computer-aided topology optimization in structural mechanics. *Structural Multidisciplinary Optimization*, pp. 90–108, 2001, DOI: 10.1007/s001580050174.
- [8] Trautmann, L.: Product customization and generative design. *Multidiszciplináris Tudományok*, Vol. 11, No. 4, pp. 87–95., DOI: <https://doi.org/10.35925/j.multi.2021.4.10>

APPLICATION OF TOPOLOGICAL METHODS

KRISTÓF SZABÓ

*University of Miskolc, Department of Machine Tools
3515 Miskolc-Egyetemváros
szabo.kristof@uni-miskolc.hu*

Abstract: The following article briefly summarizes the design aids currently in use, such as topology optimization and generative design, which are common in integrated CAD systems. The results provided by these methods are presented and compared based on a case study.

Keywords: *machine design, design theory, topology optimisation, generative design*

1. INTRODUCTION

When creating machines and structures, the design task can be done in different ways. These methods include the knowledge and steps of design methodology developed in the last century and goes under continuous development. Various procedures and techniques related to the University of Miskolc play an important role in terms of machine design [1], [4]–[7]. Each design method has its own advantages and disadvantages, but the most appropriate one is determined by the qualification of the design staff and the type of task in question. The process is greatly influenced by its resource requirements, but efforts must be made to maintain the technical and technological level of the present age and to create the best use of it. It can be observed that in many areas of industry, the proportion of human labour is decreasing compared to the work of machinery and other means of production. This is inherent in the development process, in the hope of which we can provide a solution to a given task faster, more accurately and, if necessary, at less cost. A system where one merely communicates information and makes decisions while the equipment is working, seems to be a favourable way. Similar processes are taking place in the field of product design, thanks to the generative design module that is widespread in integrated CAD systems, which serves as an example of the philosophy mentioned above. Design engineering is limited to providing accurate information and selecting from the results obtained.

2. PRESENTATION OF THE REFERENCE PART

The case study demonstrates the design of a component made up of simple geometric elements using the design methods provided by the present age, such as generative

design. The initial part is a console, which is screwed to a specific plane. A load can be hung in the mortise in the part, so the console is subjected to tensile stress.

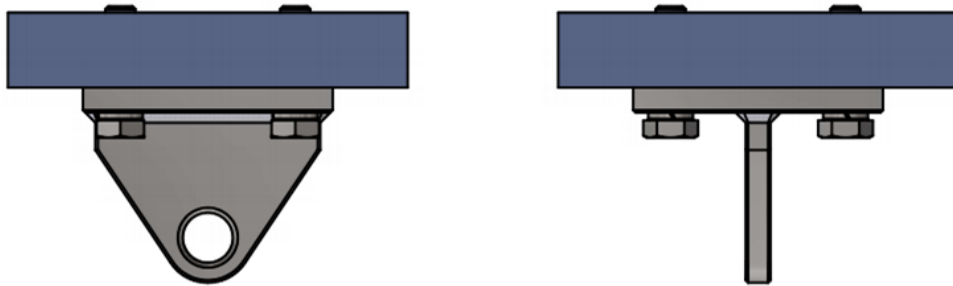


Figure 1. Installation of the reference part

It can be clearly seen in *Figure 1* that the part is fixed to the horizontal plane with four M12 screws. During the test, it is assumed that the screw connection used is suitable to withstand the resulting stress states. A hook or pin can be inserted into the hole in the bottom of the part. The console consists of two 10 [mm] thick plates joined together by a welded joint. When creating the model, the effect of the welded joint is neglected.

*Table 1
Material properties of the part*

Material properties	
Name	stainless steel 1.4125
Yield point	689 [MPa]
Tensile strength	861.25 [MPa]
Young modulus	206.7 [GPa]
Poisson factor	0.27 [-]
Shear modulus	83900 [MPa]
Density	7.75 [g/cm ³]

In order to make the results comparable, a preliminary finite element simulation is performed on the initial workpiece, so that the load capacity of the part becomes known. For finite element analysis, we used Autodesk Inventor. During the test, the value of the maximum stress and the maximum displacement due to the fact that the load is sought.

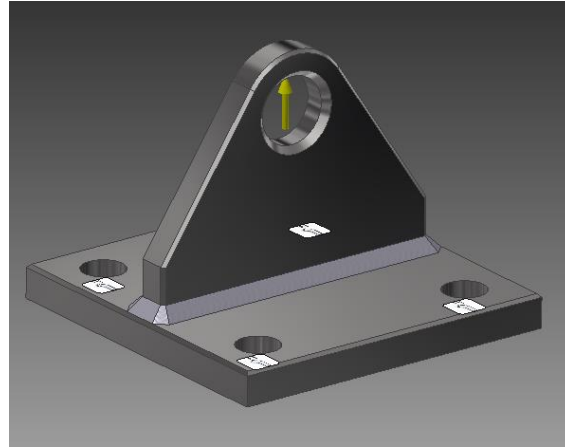


Figure 2. Place of the load and fixing points

The point and direction of application of the load applied to the component is indicated by the yellow arrow in Figure 2. From the point of view of component geometry, the direction of the specified load is considered to be critical. The load is considered static with a magnitude of 50 [kN]. The preparation of the part continues with the determination of the fixing points, which are defined at the centres of the mortises, which are symbolized by the white padlocks shown in the figure.

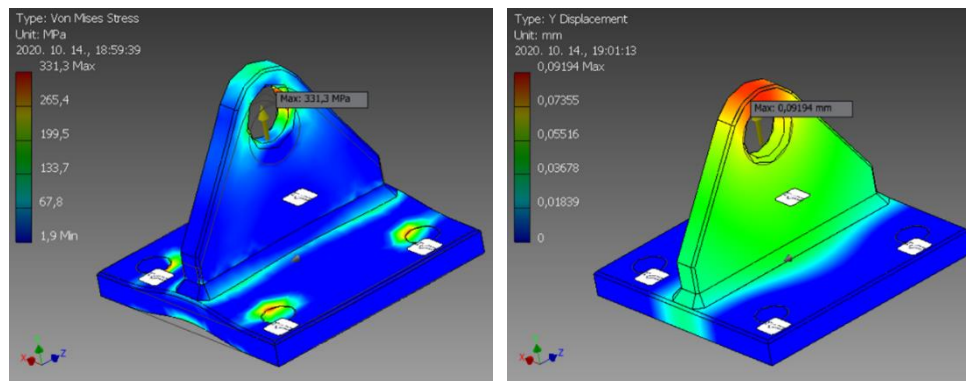


Figure 3. Stress and deformation state on the reference part

Based on the results of the study, shown on Figure 3, the maximum stress measured in the reference model under the influence of the load force is 331.3 [MPa] and the maximum displacement is 0.091 [mm].

3. APPLICATION OF TOPOLOGY OPTIMIZATION

Topological optimization requires a preliminary body model provided in the present study by the modified geometry of the reference part [8]–[11].

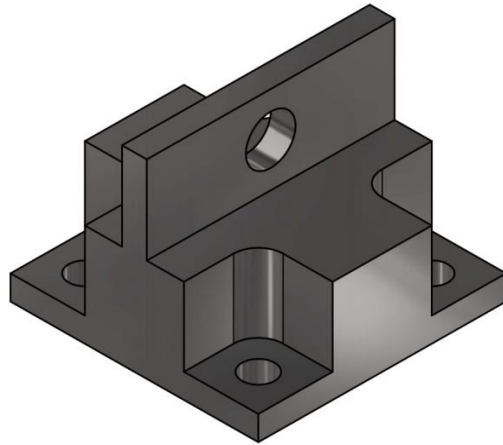


Figure 4. Modified model of the reference part

The modifications are shown in *Figure 4*, which overall increased the volume of the original model, taking care of not to interfere with the performance of the functions and to allow the installation tasks to be performed properly. The material selected during the operation is the same as the 1.4125 (440C) stainless steel used so far. In a similar way, a loading force of 50 [kN] was applied, the direction of which was unchanged. In the following, the fixing points are determined, which are the same as the previously used ones. Due to the individual mortises, it is necessary to define so-called fixed volumes, which remain unchanged solid bodies during the optimization [2], [4]. In order to obtain comparable results, it should be considered to give fixed volumes with the same parameters during topological optimization and generative design. This practically meant that cylinders with a diameter of 20 [mm] were fixed for the mortises with a diameter of 13 [mm] and a cylinder with a diameter of 36 [mm] for the mortise with a diameter of 20 [mm]. These solutions are illustrated with green bodies. The software allows the specification of a plane of symmetry or minimum network settings, the proper selection of which can reduce the computation time.

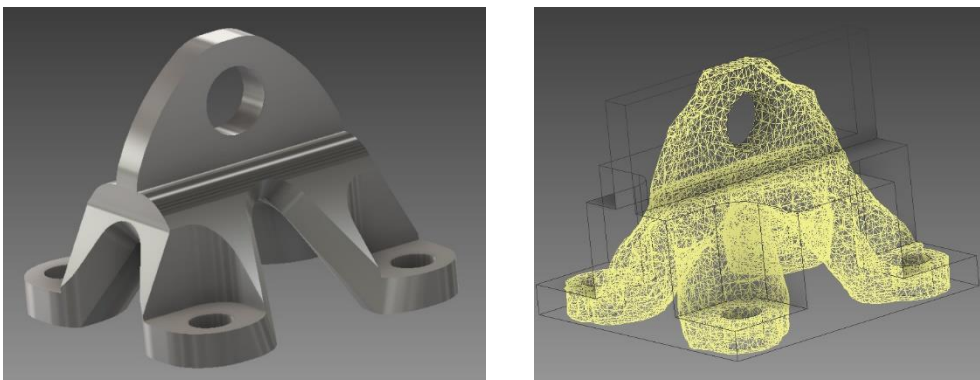


Figure 5. The result of topological optimization

Figure 5 shows the results of the optimization process. During the design, we set the weight reduction as an optimization goal, the value of which can be given in percentage. The results were obtained with a weight reduction of 13% compared to the original model, corresponding to a part weight of 0.91 [kg]. The networked model shows that the surface is very uneven. For machining by cutting, the individual ranges were approximated by planes. One of the most important aspects is whether the formed geometry is suitable to withstand the desired loads. In the following, we search for the answer to the given question using finite element simulation.

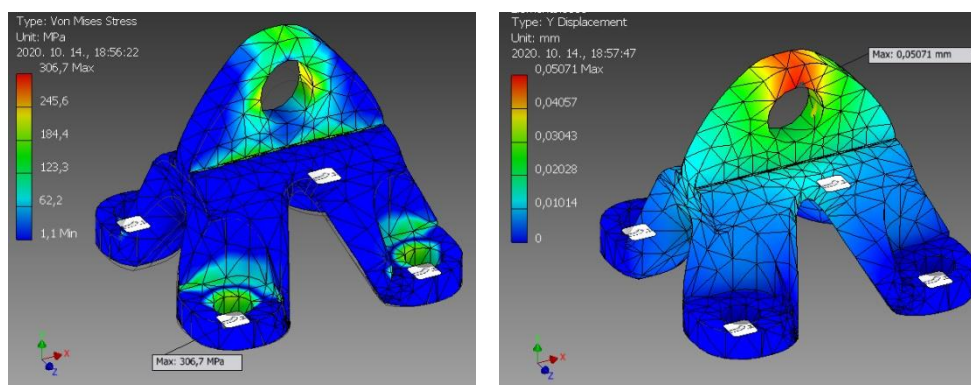


Figure 6. Stress and deformation state on the optimized part

Figure 6 shows that the maximum stress generated by the load is 306.7 [MPa], which is adequate for the safety factor used. The maximum value of the deformation is 0.05 [mm].

4. PRODUCTION OF THE PART BY GENERATIVE DESIGN

In the next section of the article, the process of constructing the part produced by the generative design method and the evaluation of the obtained results are presented. Preparations for the process, such as modelling and recording design, non-design, and fixed volumes, were made in Autodesk Inventor, and then the generative design module was applied in Autodesk Fusion 360. We have to go through a substantially similar process as with topological optimization. The individual settings are fully in line with those previously used, so that the geometry limiting the design, the material to be used, the constraint and the magnitude and direction of the load force are the same as the previously defined parameters. Once the appropriate values have been set, a check function must be started in the next step. It goes through the settings and report any deficiencies or inconsistencies to the user of the program [2], [3]. The software will notify the user if not all entered properties of the material are properly defined, or if we have not selected a suitable material for the selected machining. It is a good idea to run a preview command to check that the design volumes are selected correctly for more complex parts. After these control functions, the design

process can be started, which takes place entirely in a cloud-based storage. Accordingly, the computer can even be turned off after startup.

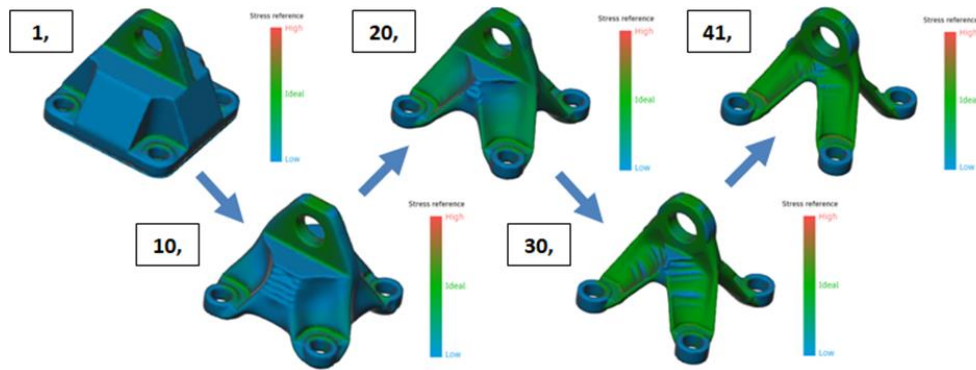


Figure 7. Iteration steps of the generation process

It is worth mentioning that many materials and manufacturing technologies can be selected, so the number of solutions is quite large. It is advisable to filter the various solutions as soon as possible. If the generation of solutions starts in a certain direction, it should be treated as a component, so after opening the result of iterations on that logical thread can also be viewed and treated as a possible solution. It may be that the direction of solution generation is favourable for us, but the final result does not fully meet the expectations, then an intermediate element of the process can be used. *Figure 7* shows the evolution of the components undergoing iteration. It is possible to monitor the stress state, which allows us to obtain information concerning the mechanical properties of the given iteration results without further investigation.

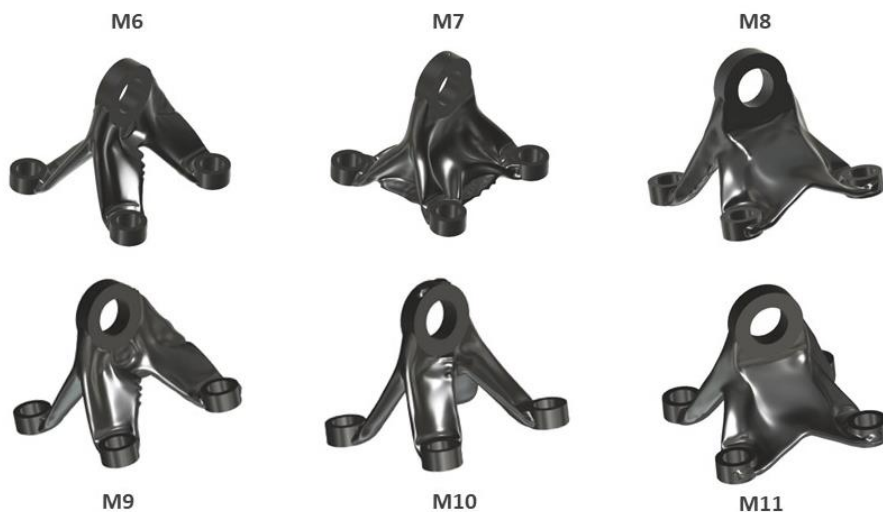


Figure 8. Results of the generative design process

The course of the generation resulted in six components shown in *Figure 8*, during which the software mapped two hundred and thirty iteration steps, each of which is a complete component. In the next step, the most suitable variant was selected. The program has a built-in comparison function in which different conditions can be assigned to each coordinate axis and the program evaluates every solution.

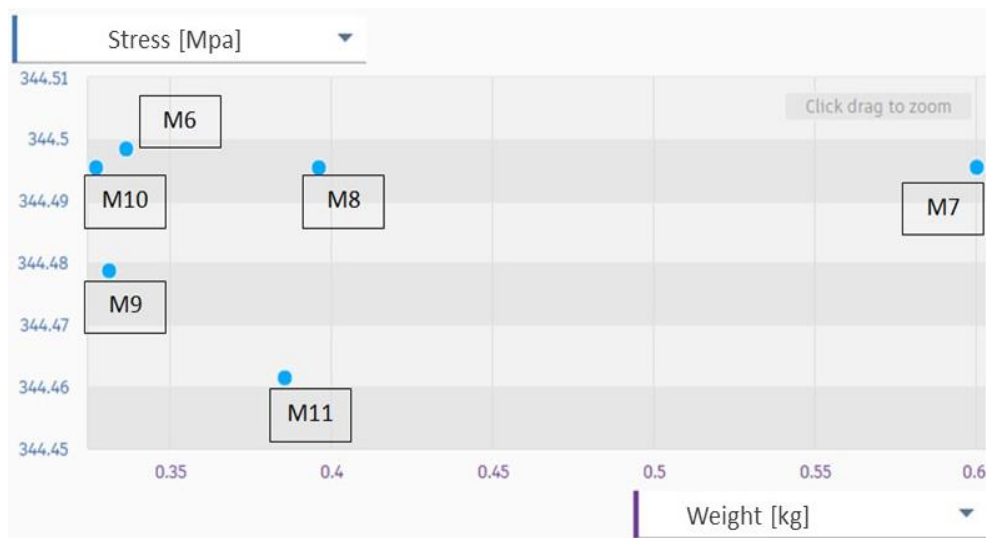


Figure 9. Classification based on stress condition and mass

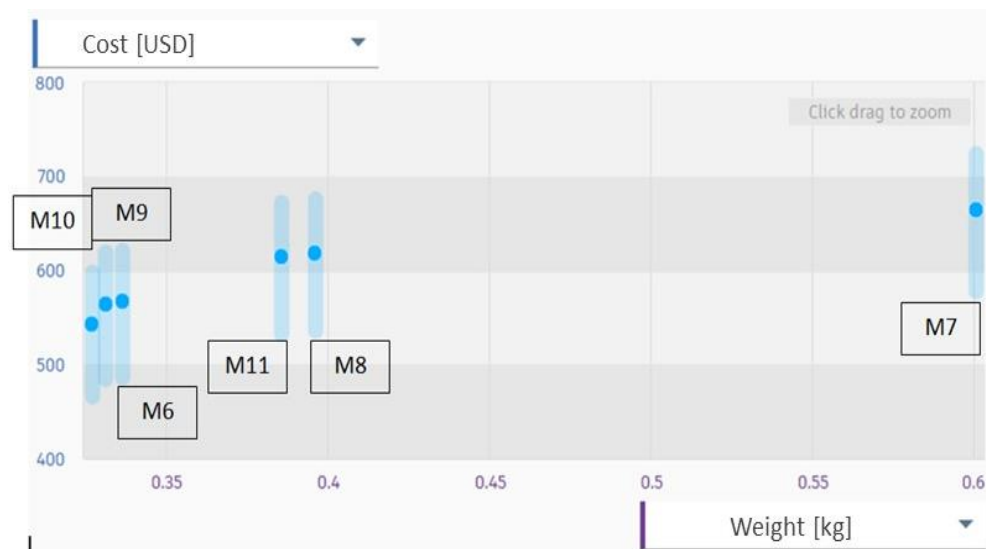


Figure 10. Classification based on production cost and weight

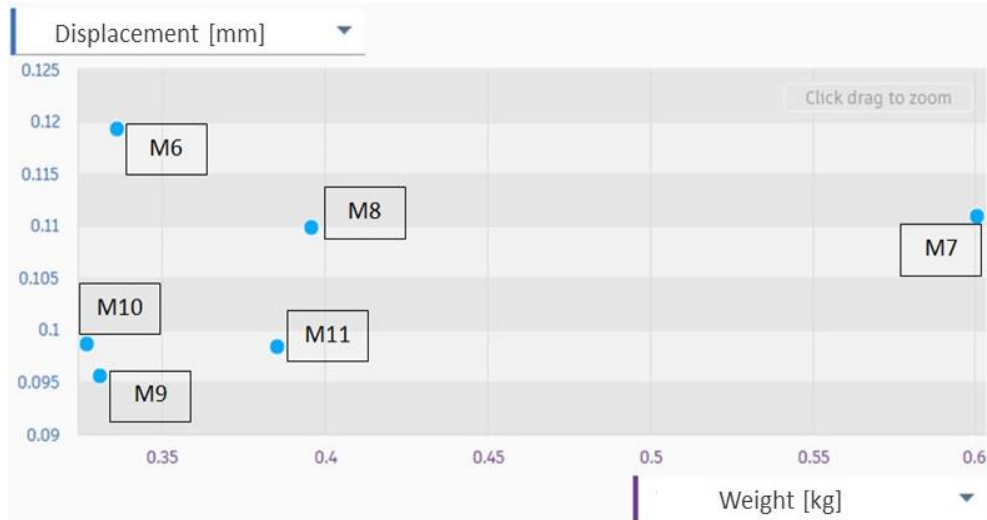


Figure 11. Classification based on deformation and mass

Based on the evaluation (Figures 9–11), the M9 and M10 solutions proved to be similarly advantageous constructs. They show a minimal difference based on the maximum displacements, on the other hand the weight and manufacturing cost of the M10 solution are lower. Accordingly, for the part produced using the generative method, the selected construction fell on the serial number M10. Based on the results obtained during the study, Table 2 summarizes the properties of the components created by the different methods.

Table 2
Summary of the results

	Traditional design	Topology optimization	Generative design
Quantity	Large series	Small series	Unique
Variations	1 [pc]	1 [pc]	230 [pc]
Machining	Cutting and welding	Milling	Additive manufacturing
Strength	331 [MPa]	306 [MPa]	344 [MPa]
Deformation	0.09 [mm]	0.05 [mm]	0.09 [mm]
Weight	1.07 [kg]	0.91 [kg]	0.32 [kg]
Weight loss	0%	17%	70%
Amount of waste	Medium	Big	Minimal
Cost	10,000 HUF	50,000 HUF	200,000 HUF

5. SUMMARY

The case study provides an insight into the process and issues of contemporary product design. The article makes a comparison of three components that use different methods, in different software, but meet the same boundary conditions. The component designed by the classical method is suitable if the product is to be produced in large series and weight reduction is not important. The production of a part designed using topological optimization is realized on a multi-axis milling machine, the productivity of which is significantly lower compared to the traditional design. The amount of waste generated during production is high, so the use of a component designed in this way is recommended for small series, where the additional advantage is weight reduction. In many cases, the production of a component designed by the generative design method can only be carried out with additive technology, which has low productivity but high cost. The positive thing about production is that waste generation is low. Thus, the use of the generative design method is recommended when achieving significant weight reduction or when using difficult-to-cut materials.

ACKNOWLEDGEMENT

The described article/presentation/study was carried out as part of the EFOP-3.6.1-16-00011 *Younger and Renewing University – Innovative Knowledge City – institutional development of the University of Miskolc aiming at intelligent specialisation* project implemented in the framework of the Szechenyi 2020 program. The realization of this project is supported by the European Union, co-financed by the European Social Fund.

REFERENCES

- [1] Takács, Gy. – Zsiga, Z. – Szabóné Makó I. – Hegedűs, Gy.: *Gyártóeszközök módszeres tervezése*. Nemzeti Tankönyvkiadó, Miskolc, 2011.
- [2] Szabó, K. – Hegedűs, Gy.: A generatív tervezés lépései integrált CAD rendszerekben. *Multidiszciplináris Tudományok*, Vol. 10, Nr. 4, 2020, pp. 393–398, DOI: 10.35925/j.multi.2020.4.43.
- [3] Szabó, K. – Hegedűs, Gy.: Brief Overview of Generative Design Support Software. *Design of Machines and Structures*, Vol. 10, No. 2, pp. 123–132., 2020, DOI: 10.32972/dms.2020.023.
- [4] Hegedűs, Gy. *A módszeres géptervezés alkalmazása ipari mérőgép fejlesztése estén*. Doktoranduszok Fóruma 2002: Gépészmérnöki Kar szekciókiadványa, Miskolci Egyetemi Kiadó, 2002, Miskolc
- [5] Kamondi, L. – Sarka, F. – Takács, Á.: *Fejlesztés-módszertani ismeretek*. Nemzeti Tankönyvkiadó, Miskolc, 2011.
- [6] Takács, Á.: Computer Aided Concept Building. *Solid State Phenomena*, Vol. 261, 2017, pp. 204–207, DOI: 10.4028/www.scientific.net/SSP.261.402.

-
- [7] Pahl, G. – Beitz, W. – Feldhusen – Grote, K.-H.: *Engineering Design – A Systematic Approach*. Springer-Verlag, London, 2007, ISBN 978-1-84628-318-5.
- [8] Stejskal, T. – Dovica, M. – Svetlík, J. – Demec, P. – Hrivniak, L. – Šašala, M.: Establishing the Optimal Density of the Michell Truss Members. *Materials*, Vol. 13, No. 17, 2020, pp. 12–17, DOI: 10.3390/ma13173867.
- [9] Zuo, K. – Chen, L. – Zhang, Y. – Yang, J.: Study of key algorithms in topology optimization. *International Journal of Advanced Manufacturing Technology*, Vol. 32, No. 7–8, 2007, pp. 787–796, DOI: 10.1007/s00170-005-0387-0.
- [10] Bendsøe, M.: *Optimization of Structural Topology, Shape and Material*. Springer Verlag, Berlin, 1995, DOI: 10.1007/978-3-662-03115-5.
- [11] Trautmann, L.: Product customization and generative design. *Multidiszciplináris Tudományok*, Vol. 11, No. 4, 2021, pp. 87–95, DOI: <https://doi.org/10.35925/j.multi.2021.4.10>.

REVIEWING COMMITTEE

- L. CZÉGÉ
Department of Mechanical Engineering
Faculty of Engineering
University of Debrecen
H-4028 Ótemető street 2–4, Debrecen
czege.levente@eng.unideb.hu
- CS. DÖMÖTÖR
Institute of Machine and Product Design
University of Miskolc
H-3515 Miskolc-Egyetemváros, Hungary
machdcs@uni-miskolc.hu
- M. MÁTÉ
Mechanical Engineering Department
Sapientia Hungarian University of Transylvania
Faculty of Technical and Human Sciences Târgu-Mureş
540485 Târgu-Mureş, Op. 9., Cp. 4, Romania
mmate@ms.sapientia.ro
- L. RÓNAI
Institute of Machine Tools and Mechatronics
University of Miskolc
H-3515 Miskolc-Egyetemváros, Hungary
ronai.laszlo@uni-miskolc.hu
- F. SARKA
Institute of Machine and Product Design
University of Miskolc
H-3515 Miskolc-Egyetemváros, Hungary
machsf@uni-miskolc.hu
- T. SZABÓ
Institute of Machine Tools and Mechatronics
University of Miskolc
H-3515 Miskolc-Egyetemváros, Hungary
mrbszabo@uni-miskolc.hu
- Á. TAKÁCS
Institute of Machine and Product Design
University of Miskolc
H-3515 Miskolc-Egyetemváros, Hungary
takacs.agnes@uni-miskolc.hu
- Á. TÖRÖK
KTI – Institute for Transport Sciences
H-1119 Budapest,
Than Karoly street 3–5, Hungary
torok.adam@kti.hu

Responsible for the Publication: Prof. dr. Zita Horváth
Published by the Miskolc University Press under leadership of Attila Szendi
Responsible for duplication: Works manager: Erzsébet Pásztor
Editor: Dr. Ágnes Takács
Technical editor: Csilla Gramantik
Proofreader: Zoltán Juhász
Number of copies printed: 50
Put the Press in 2021
Number of permission: MERT – 2021 – 85 – ME
HU ISSN 1785-6892 in print
HU ISSN 2064-7522 online